TIME-REVERSIBLE OPERATOR COMPOSITION INTEGRATOR FOR THE BERENDSEN TEMPERATURE-CONTROL MOLECULAR DYNAMICS EQUATION*

IKUO FUKUDA†, SÉVERINE QUEYROY‡, AND HARUKI NAKAMURA†

Abstract. The Berendsen equations of motion (EOM) are widely used for controlling the temperature of a target physical system in molecular dynamics (MD) simulation. In spite of the usefulness of the Berendsen EOM, its numerical integration has never raised much attention mainly due to its non-Hamiltonian feature. Nevertheless, a non-optimal integration scheme definitely limits the possibility of its applications. In order to efficiently integrate the Berendsen EOM, we construct here an operator composition scheme that has the following properties: First, the scheme is symmetric, i.e., it is time reversible as is the original differential equation; Second, the scheme is systematic, i.e., any higher order of the local accuracy can be attained by a composition method; Third, the scheme is robust, i.e., a velocity scaling factor that is bounded with respect to $s = h/\tau$ was obtained and thus allows a larger s. Here h is the unit time step of the integration and τ is the EOM parameter related to the temperature-control speed (faster for a smaller τ). These good properties were confirmed, with a comparison to conventional methods, by applying them into an isolated ethane molecule, a bulk argon system, and a bulk ethane system. Our extended EOM formalism, which provides an invariant function, also helps to observe the numerical error that cannot be detected solely by the temperature controllability.

Key words. Berendsen equations of motion, molecular dynamics, temperature control, numerical integration, time reversibility, symmetric composition, invariant function

AMS subject classification. 65L05, 65Y04, 81V55

1. Introduction. Temperature control in molecular dynamics (MD) method [1, 2] is important to conduct a realistic simulation of a physical system [3, 4]. There are many algorithms to control the temperature of a given physical system, and they are called thermostat methods [5, 6, 7].

Among them, the Nosé-Hoover (NH) thermostat method [8, 9] can generate the Boltzmann-Gibbs distribution at the target temperature under the assumption of the ergodicity. The structure of the NH equation is basically simple and universal, which allows many extensions (see e.g., Refs. [10, 11, 12, 13] for recent work and the references in [6, 14] for earlier work). The NH equation is obtained by adding a force of the form $-\zeta v$ to the Newtonian equations of motion (EOM) that the original physical system, defined by coordinate x and velocity v, should obey. Here, the friction coefficient-like quantity is a dynamical variable developing according to $\zeta(t) \propto \int_0^t (K(v(t'))/K_0 - 1)\,\mathrm{d}t' + \text{const.}$, where $K(v)$ and K_0 are the present and target values of the kinetic energy of the physical system, with t being a time. In this sense the NH equation is based on the "integral" scheme [15] for controlling the temperature, or the kinetic energy, where the deviation $K(v)/K_0 - 1$ is integrated with respect to time (we consider the instantaneous temperature and the kinetic energy to be proportional).

The Gaussian isokinetic method [16, 17, 18, 19] fixes the temperature of the system as the initial value with suppressing the deviations. This is based on the Gauss's constraint method, which can be viewed as the "differential" control scheme [15],

*Dated: 19 February 017

†Institute for Protein Research, Osaka University, Osaka 565-0871, Japan (correspondence should be addressed: ifukuda@protein.osaka-u.ac.jp)

‡Aix Marseille Univ, CNRS, ICR, Marseille, France. The part of the work was performed during a stay of Q.S. in Osaka University by the support of the International Joint Research Promotion Program.

since it is defined by the Newtonian EOM attaching the frictional force $-\zeta v$ with $\zeta(t) \propto -\frac{\mathrm{d}}{\mathrm{d}t}U(x(t))$, where $U(x)$ is the potential energy of the physical system.

Berendsen *et al.* [20] proposed an alternative method to control the temperature, based on a "direct" control scheme. This is defined in the same manner as the above methods but uses $\zeta(t) \propto (1 - K_0/K(v(t)))$ without integration or differentiation. Despite the ambiguity of the phase-space distribution produced [21], the Berendsen method is simple, stable, intuitive, and has been employed by many users [22] for e.g. biological simulations. In fact, the simplicity of the method allows to combine it with a grand canonical MD [23] and with dissipative particle dynamics [24]. The stability of the method allows to effectively equilibrate a roughly prepared system or to perform a subtle temperature change, even though other elaborated schemes fail. The Berendsen method, as well as the NH method and the stochastic velocity re-scaling method [25], yield transport properties that are statistically indistinguishable from that under the microcanonical ensemble, while the diffusion properties are significantly dampened by the Andersen thermostat and Langevin dynamics, when strong coupling is used [26].

In spite of the usefulness of the Berendsen equation, its numerical integration has never raised much attention. The system is not a Hamiltonian system [27, 28], so one cannot directly use symplectic integrators [29, 30, 31, 32, 33], which has been shown to be efficient in a variety of studies [34, 35, 36]. This was the main reason to hamper the development of an efficient numerical integration based on a theoretically clear foundation. Most of the integration algorithms for the Berendsen EOM are thus based on heuristic approaches, obtained by a combination of the leapfrog method and the velocity scaling, which may give $\mathcal{O}(\Delta t)$ accuracy. However, these approaches lack both the time-reversibility feature and a protocol to attain high accuracy. Another reason to prevent the development of an efficient integrator may be originated to the purpose of the use. That is, one often supposes that it is sufficient to have a good temperature controllability of the target physical system and that the accuracy is of second importance. However, there are cases where the temperature control is good but a large numerical error is accumulated. Thus a method to capture the error is necessary to get physically correct results.

In this paper we propose a time-reversible (symmetric) integrator of the Berendsen EOM, where the EOM is extended so as to have a time invariant function. These devices are based on the techniques previously developed for non-Hamiltoninan systems [37]. From the time reversibility, the integrator map preserves the reversible feature that the original ordinary differential equation (ODE) has. This should contribute to the accurate integration [38]. By monitoring the value of the constructed invariant function, numerical integration on the extended space can be done without destroying the original solutions of the ODE and will detect the error that cannot be necessarily done by the temperature controllability. The integrator is explicit, and furthermore, higher-order integrators can be systematically constructed by the symmetric operator composition technique, which is based on an effective splitting of the target vector field [39]. It should also be noted that the exact operator map leads to a robustness of the current method. That is, the current method uses a velocity scaling factor that is bounded with respect to timestep, while conventional methods use a scaling factor that is unbounded, leading to instabilities. Similarities and differences between the current and conventional methods are revealed theoretically in depth and numerically using molecular systems. We believe the current study to be the first one to discuss both the Berendsen's method and the integrator mathematics.

Section 2 reviews the Berendsen EOM and its integration schemes found in the

literature. In section 3, we present our integration scheme and demonstrate its fundamental properties. In section 4 we theoretically discuss relationships between the current and the conventional integration methods. Their mathematical details are demonstrated in Appendixes A and B. In section 5, we investigate properties of the current method and compare it with other methods, via numerical simulations using one model system and two bulk atom/molecule systems. Section 6 summarizes the current work and gives remarks.

2. Berendsen equations of motion. The Berendsen EOM can be represented by [20],

$$\left.\begin{aligned} \dot{x} &= v, \\ \dot{v} &= F(x)\mathbf{M}^{-1} + \frac{1}{2\tau}\left(\frac{K_0}{K(v)} - 1\right) v, \end{aligned}\right\} \tag{2.1}$$

where $x \equiv (x_1, \ldots, x_n) \in D \subset \mathbb{R}^n$, $v \equiv (v_1, \ldots, v_n) \in \mathbb{R}^n$, $F(x) \in \mathbb{R}^n$, and $K(v) \equiv \sum_{i=1}^{n} m_i v_i^2/2$ represent the atomic coordinates, velocities, force (smooth vector-valued function on a domain D), and kinetic energy, respectively, of a physical system of n degrees of freedoms, with m_i being a mass parameter, which defines the matrix $\mathbf{M} \equiv \mathrm{diag}(m_1, ..., m_n)$. The friction-coefficient variable $\zeta \equiv -\frac{1}{2\tau}\left(\frac{K_0}{K(v)} - 1\right)$ governs the control of the temperature of a physical system, $T(v) \equiv 2K(v)/nk_\mathrm{B}$, referring to the target temperature $T_0 \equiv 2K_0/nk_\mathrm{B} > 0$, (viz., K_0 is the target kinetic energy value), with k_B being Boltzmann's constant. The parameter (time constant) $\tau > 0$ adjusts the control strength, where a large τ gives a weak control, and the limit $\tau \to \infty$ reduces to the Newtonian equations of motion. Note that a similar but alternative definition of ζ is discussed in [40].

Typical numerical integration schemes to solve the EOM are the following. In the original approach [20, 22], the present-timestep coordinates and velocities (x', v') are obtained from the one-timestep-preceding quantities (x, v) as:

$$\tilde{v} = v + hF(x)\mathbf{M}^{-1} \tag{2.2a}$$

$$v' = \lambda_h(v)\tilde{v}, \tag{2.2b}$$

$$x' = x + hv', \tag{2.2c}$$

where h indicates the unit time step used in the integration. Here,

$$\lambda_h(v) \equiv \left[1 + \frac{h}{\tau}\left(\frac{K_0}{K(v)} - 1\right)\right]^{\frac{1}{2}} \tag{2.3}$$

is the scaling factor of the atomic velocity for the temperature control [20]. Note that another definition of the present-timestep velocity, which keeps the original integration scheme given by (2.2), is possible, such as $(v' + v)/2$. Equation (2.2) is considered to be a first-order algorithm (see section 4.2), and we denote it by Method 1 for the reference. Alternatively, we can use a slightly modified version where $\lambda_h(\tilde{v})$ is used instead of $\lambda_h(v)$ in (2.2b), and we call this a modified Berendsen scheme or, simply, Method 1 mod. Note that the original paper [20] uses $T_0/T(v)$, the ratio of the target temperature and the present temperature, instead of $K_0/K(v)$, and considers the linear transformation such as $T(v) = 2K(v)/k_\mathrm{B}(3N - N_\mathrm{c} - 3)$, with N being the number of atoms and N_c being the number of constraints. We see that $K_0/K(v) = T_0/T(v)$ irrespective of the linear transformation, so that (2.1) and (2.3) are suitable.

As considered in Khalili *et al.* [41], the velocity scaling and the Verlet scheme can be combined such as

$$x' = x + hv + \frac{h^2}{2}F(x)\mathbf{M}^{-1}, \tag{2.4a}$$

$$\tilde{v} = v + \frac{h}{2}(F(x) + F(x'))\mathbf{M}^{-1} \tag{2.4b}$$

$$v' = \lambda_h(\tilde{v})\tilde{v}. \tag{2.4c}$$

Namely, after the velocity Verlet algorithm, the scaling is done; we call it Method 2. An alternative choice is to use $\lambda_h(v)$ instead of $\lambda_h(\tilde{v})$ in (2.4c).

3. Extended system and integration scheme.

3.1. Extended ODE and invariant. The simple scheme [37] to construct an invariant function is briefly reviewed in section 3.1.1, and it is applied to the Berendsen EOM in section 3.1.2.

3.1.1. General scheme. For a given arbitrary smooth ODE in a domain Ω of $\mathbb{R}^N$,

$$\dot{\omega} = X(\omega), \tag{3.5}$$

we associate an additional variable $\mathrm{v} \in \mathbb{R}$ to the original variables $\omega = (\omega_1, \ldots, \omega_N) \in \Omega$ and represent them by $\omega' = (\omega, \mathrm{v})$ as a point of an "extended space" $\Omega' \equiv \Omega \times \mathbb{R}$. We then make an "extended ODE" [37] on Ω',

$$\dot{\omega}' = X'(\omega'), \tag{3.6}$$

which is defined by

$$\dot{\omega} = X(\omega), \tag{3.7a}$$

$$\dot{\mathrm{v}} = Y(\omega). \tag{3.7b}$$

Here $Y : \Omega \to \mathbb{R}$ is an extended-field function defined by

$$\begin{aligned} Y(\omega) &\equiv -(X(\omega)|\nabla B(\omega)) \\ &= -\sum_{i=1}^{N} X_i(\omega)\, D_i B(\omega), \end{aligned} \tag{3.8}$$

with B being an arbitrary smooth function on Ω. It is then shown that a function

$$L : \Omega' \to \mathbb{R},\ \omega' \overset{\mathrm{d}}{\mapsto} B(\omega) + \mathrm{v} \tag{3.9}$$

becomes an invariant of the extended ODE; i.e., for an arbitrary solution $\phi' \equiv (\omega, \mathrm{v})$ of (3.6),

$$L(\phi'(t)) = B(\omega(t)) + \mathrm{v}(t) \tag{3.10}$$

is constant for any time t. Thus, by monitoring the conservation of the invariant while numerically integrating the extended ODE, we can check the numerical error. It is clear that all solutions, $t \mapsto \omega(t)$, in the original ODE (3.7a) are unaffected by adding v and its EOM (3.7b).

3.1.2. For the Berendsen EOM. According to the scheme, for the Berendsen ODE (2.1)

$$\dot{\omega} = X_{\mathrm{B}}(\omega), \tag{3.11}$$

where

$$X_{\mathrm{B}} : \Omega \to \mathbb{R}^{2n},\ \omega \equiv (x, v) \mapsto \left(v,\ F(x)\mathbf{M}^{-1} + \frac{1}{2\tau}\left(\frac{K_0}{K(v)} - 1\right) v \right)$$

with $\Omega \equiv D \times \mathbb{R}^n_\times$ [viz., all (x, v) except $v = 0 \in \mathbb{R}^n$], the extended ODE is defined by

$$\begin{aligned} \dot{\omega}' &= X'_{\mathrm{B}}(\omega') \in \mathbb{R}^{2n+1} && \text{(3.12a)} \\ &= (X_{\mathrm{B}}(\omega), Y(\omega)) && \text{(3.12b)} \\ &= \left(v,\ F(x)\mathbf{M}^{-1} + \frac{1}{2\tau}\left(\frac{K_0}{K(v)} - 1\right) v,\ Y(\omega) \right), && \text{(3.12c)} \end{aligned}$$

viz.,

$$\left.\begin{aligned} \dot{x} &= v, \\ \dot{v} &= F(x)\mathbf{M}^{-1} + \frac{1}{2\tau}\left(\frac{K_0}{K(v)} - 1\right) v, \\ \dot{\mathrm{v}} &= Y(\omega) = -(X(\omega)|\nabla B(\omega)), \end{aligned}\right\} \tag{3.13}$$

and the invariant is $L(\omega, \mathrm{v}) = B(\omega) + \mathrm{v}$.

Among a variety of choices of the function B, the following one may be physically natural:

$$B(x, v) \equiv U(x) + K(v), \tag{3.14}$$

viz., B is the total energy of the system, where we assume the existence of the potential function U such that $F = -\nabla U$. Applying (3.14) to (3.8), we get $Y(\omega) = \frac{1}{\tau}\left(K(v) - K_0\right)$ and so have the extended equation and the invariant as follows:

$$\dot{\mathrm{v}} = \frac{1}{\tau}\left(K(v) - K_0\right), \tag{3.15}$$

$$L(\omega, \mathrm{v}) = U(x) + K(v) + \mathrm{v}. \tag{3.16}$$

We can also confirm (3.16) to be a time invariant for (3.13) by a straightforward differentiation with respect to time:

$$-(F(x(t))|v(t)) + \frac{d}{dt}K(v(t)) + \frac{1}{\tau}\left(K(v(t)) - K_0\right) = 0.$$

Interestingly, this is equivalent to the relation based on the original consideration of the "global coupling" [i.e., equation (9) in [20]]. Note also that as $\tau \to \infty$, we have the Newtonian limit: the EOM approaches the Newtonian EOM, and the invariant (3.16) approaches the Newtonian total energy $K(v) + U(x)$ up to $\mathrm{v}(0) = \mathrm{const}$.

A slightly generalized choice of B defined by

$$B(x, v) \equiv c_1 U(x) + c_2 K(v), \tag{3.17}$$

where c_1 and c_2 are parameters, produces the following EOM of v and the invariant,

$$\begin{aligned}\dot{\mathrm{v}} &= Y(\omega) \\ &= (c_1 - c_2)(F(x)|v) + \frac{c_2}{\tau}\left(K(v) - K_0\right), \qquad (3.18)\\ L(\omega, \mathrm{v}) &= c_1 U(x) + c_2 K(v) + \mathrm{v}, \qquad (3.19)\end{aligned}$$

respectively. It is pointed out that the choice of $c_1 = 0$ would be useful in the case where the potential U does not exist.

Note that Bussi *et al.* [25] proposed a stochastic canonical sampling method along the line of the velocity scaling and discussed an associated conserved quantity that is defined for an individual trajectory. The notion of this conserved quantity seems similar to that of the *extended invariant* [37] for an ODE. However, our target here is in the ODE, and the invariant is a function globally defined in the phase space, which are the differences between the approach of Bussi *et al.* and ours.

3.2. Integrator.

3.2.1. First-order Integrator. To construct a numerical integrator, we decompose a target vector field and compose the corresponding phase space maps, according to the scheme described in [37]. We decompose the target extended field X'_{B}, defined by (3.12b)–(3.12c), as $X'_{\mathrm{B}} = \sum_{i=1}^{4} X'^{[i]}$, where

$$\begin{aligned}X'^{[1]}(\omega') &\equiv (v,\, 0, 0)\,, \qquad (3.20a)\\ X'^{[2]}(\omega') &\equiv \left(0,\, F(x)\mathbf{M}^{-1}, 0,\right), \qquad (3.20b)\\ X'^{[3]}(\omega') &\equiv \left(0,\, \frac{1}{2\tau}\left(\frac{K_0}{K(v)} - 1\right) v, 0\right), \qquad (3.20c)\\ X'^{[4]}(\omega') &\equiv (0,\, 0, Y(\omega))\,. \qquad (3.20d)\end{aligned}$$

The point to get the decomposition is to ensure that each ODE

$$\dot{\omega}' = X'^{[i]}(\omega') \qquad (3.21)$$

can be solved explicitly. This is trivial for $i = 1$, 2, and 4, but may not be for $i = 3$:

$$\left.\begin{aligned}\dot{x} &= 0,\\ \dot{v} &= \frac{1}{2\tau}\left(\frac{K_0}{K(v)} - 1\right) v\\ \dot{\mathrm{v}} &= 0.\end{aligned}\right\} \qquad (3.22)$$

We find that the solution of ODE (3.22) taking an initial value $(x_0, v_0, \mathrm{v}_0) \in \Omega'$ is

$$\begin{aligned}x(t) &= x_0, \qquad (3.23a)\\ v(t) &= \left[\left(1 - \frac{K_0}{K(v_0)}\right)\exp\left(-\frac{t}{\tau}\right) + \frac{K_0}{K(v_0)}\right]^{\frac{1}{2}} v_0, \qquad (3.23b)\\ \mathrm{v}(t) &= \mathrm{v}_0. \qquad (3.23c)\end{aligned}$$

It should be stressed that $X'^{[3]}$ is a smooth (now, of class C^∞) field on Ω' so that the solution of the initial value problem is unique. Since we can directly check that (3.23) satisfies both (3.22) and $(x(0), v(0), \mathrm{v}(0)) = (x_0, v_0, \mathrm{v}_0)$, equation (3.23) is the unique

solution. Note that the decomposition of $X'_{\rm B}$ is natural in that the additional quantities v and Y do not affect the solutions of a decomposed original ODE $\dot{\omega} = X^{[i]}(\omega)$ for $i = 1$, 2, and 3, where $X^{[i]}$ is obtained by the same type of the decomposition of the original (not extended) field $X_{\rm B} = \sum_{j=1}^{3} X^{[i]}$ [viz., $X^{[i]}$ is defined by removing 0 in the last column of (3.20a), (3.20b), and (3.20c) for $i = 1$, 2, and 3, respectively]. In particular, (3.23) is not affected by v and Y.

Hence, the exact flow $\Phi_t^{[i]}$ for each vector field $X'^{[i]}$, where $t \mapsto \Phi_t^{[i]}(\omega')$ denotes the solution of (3.21) with an initial value $\omega' \in \Omega'$, is thus represented by the following map or operator on the extended phase space Ω':

$$\Phi_h^{[1]} : \omega' \mapsto (hv + x,\, v, \mathrm{v})\,, \tag{3.24a}$$

$$\Phi_h^{[2]} : \omega' \mapsto \left(x,\, hF(x)\mathbf{M}^{-1} + v,\, \mathrm{v}\right), \tag{3.24b}$$

$$\Phi_h^{[3]} : \omega' \mapsto (x,\, \Lambda_h(v)v,\, \mathrm{v})\,, \tag{3.24c}$$

$$\Phi_h^{[4]} : \omega' \mapsto (x,\, v, hY(x,v) + \mathrm{v})\,, \tag{3.24d}$$

where we have used h instead of t. Here,

$$\Lambda_h(v) \equiv \left[\left(1 - \frac{K_0}{K(v)}\right)\exp\left(-\frac{h}{\tau}\right) + \frac{K_0}{K(v)}\right]^{\frac{1}{2}} \tag{3.25}$$

comes from (3.23b) and becomes the counterpart of $\lambda_h(v)$ defined in (2.3); see the next section for their comparison and see Appendix A for their detailed properties.

Then we get a first-order integrator with an unit time step h,

$$\Phi_h = \Phi_h^{[4]} \circ \Phi_h^{[3]} \circ \Phi_h^{[2]} \circ \Phi_h^{[1]}, \tag{3.26}$$

which will be a map from Ω' to Ω' (see Appendix B for mathematical details, including the fact that the maps $\Phi_h^{[i]}$ are not necessarily defined for all $h \in \mathbb{R}$ except for $i = 4$). There are many possibilities [37] about the appearing order of $\Phi_h^{[i]}$ in (3.26), and we discuss it later. The integration scheme (3.26), defining the change from the preceding values to the present values, $(x, v, \mathrm{v}) \mapsto (x', v', \mathrm{v}')$, is also expressed in an explicit operation form,

$$x' = x + hv. \tag{3.27a}$$

$$\tilde{v} = hF(x')\mathbf{M}^{-1} + v, \tag{3.27b}$$

$$v' = \Lambda_h(\tilde{v})\tilde{v}, \tag{3.27c}$$

$$\mathrm{v}' = hY(x', v') + \mathrm{v}, \tag{3.27d}$$

and practically used in computer code. Rather than the form of these operations, the form of (3.26) expressed by the maps $\Phi_h^{[i]}$ is helpful for theoretical analyses. The latter form, which has not been taken into account in conventional studies for the Berendsen EOM though, enables us to properly grasp $\Phi_h^{[i]}$, Φ_h, and T_h, where $\Phi_h^{[i]}$ ($i = 1, \ldots, 4$) are the constituents of the integration map Φ_h, which in turn mimic the exact flow T_h for the target ODE (3.12); $\Phi_h^{[i]}$, Φ_h, and T_h are uniformly viewed as maps (operators) on Ω' and can be analyzed with certain *properties of maps* (the so-called "symplectic integrator" on a Hamiltonian system [28] is constructed in the same spirit, where the symplectic property of maps is concerned).

3.2.2. Higher-order Integrator. The viewpoint of the maps is also useful to systematically raise the (local) accuracy of the integrator. In fact, an integrator with second-order accuracy can be constructed as a map by composing maps based on Φ_h, which is of the first-order accuracy. Here, an integrator map Ψ_h is said to be pth-order, if

$$T_h(\omega') - \Psi_h(\omega') = \mathcal{O}(h^{p+1}) \tag{3.28}$$

holds for any ω'. A typical second-order integrator is an extended version of the Verlet method [37, 42]:

$$\Psi_h = \Phi_{h/2} \circ \Phi^*_{h/2}, \tag{3.29}$$

where

$$\Phi^*_t \equiv (\Phi_{-t})^{-1} \tag{3.30a}$$

$$= \Phi^{[1]}_h \circ \Phi^{[2]}_h \circ \Phi^{[3]}_h \circ \Phi^{[4]}_h \tag{3.30b}$$

is the adjoint map of Φ_t and also a first-order integrator. Thus we have

$$\Psi_h = \Phi^{[4]}_{h/2} \circ \Phi^{[3]}_{h/2} \circ \Phi^{[2]}_{h/2} \circ \Phi^{[1]}_h \circ \Phi^{[2]}_{h/2} \circ \Phi^{[3]}_{h/2} \circ \Phi^{[4]}_{h/2}. \tag{3.31}$$

Equations (3.30b) and (3.31) can be automatically derived from the fact that each map $\Phi^{[i]}_h$ is the exact flow [of the decomposed ODE (3.21)]. The explicit forms of operations for Ψ_h are provided by the similar manner as (3.27).

The appearance ordering of $\Phi^{[j]}_h$ ($j = 1, \ldots, 4$) in (3.26) is arbitrary to ensure the first-order local accuracy. However, the ordering has an influence on the computational time needed. The most time-consuming operand in (3.24) is the evaluation of force $F(x)$ or potential $U(x)$. The force evaluation is required for $\Phi^{[2]}_h$. In addition, the evaluation of $F(x)$ or $U(x)$ may be required for $\Phi^{[4]}_h$ (function Y) and for the invariant. Here, specifically consider the typical integration form (3.29). Then, the number of the force or potential evaluation is 1 (viz., the minimum) for any cases if we use the ordering of (3.26), but otherwise it may be 2. Details are discussed in section I of Supplementary materials. For these reasons, one of our recommended ordering, for any Y, is given by (3.26).

Now, using the first-order maps defined by (3.26) and (3.30), higher-order integrators can be obtained as a map by the symmetric composition with the adjoint [43]:

$$\Psi_h = \Phi_{\alpha_s h} \circ \Phi^*_{\beta_s h} \circ \cdots \circ \Phi_{\alpha_2 h} \circ \Phi^*_{\beta_2 h} \circ \Phi_{\alpha_1 h} \circ \Phi^*_{\beta_1 h}, \tag{3.32}$$

where coefficients $\{\alpha_i, \beta_i\} \subset \mathbb{R}$ satisfy the symmetric condition

$$\alpha_i = \beta_{s+1-i},\ i = 1, ..., s, \tag{3.33}$$

in order to satisfy the symmetric property: $\Psi^*_h = \Psi_h$ [see also section 4.3 (ii)]. Specific values of the parameters, viz., stage s and coefficients $\{\alpha_i, \beta_i\}$, as described in [42], can be used, and we have presented several second-order integrators (they are designated as P2S1 or P2S2 [43, 44]) and fourth-order integrators (P4S5 [44] and P4S6 [45]). Among second-order integrators, the simplest one is called as P2S1, defined by (3.29):

$$\Psi^{\mathrm{P2S1}}_h = \Phi_{h/2} \circ \Phi^*_{h/2}$$

Note that a volume preserving integrator can be constructed according to the current scheme with the twisting technique described in [37].

4. Relationship among the integrators.

4.1. Reinterpretation of conventional methods. To observe the relationship between the current and the conventional integration methods, we first consider the velocity scale factors $\Lambda_h(v)$ and $\lambda_h(v)$, which are given by (3.25) and (2.3), respectively. They are intimately related with each other. As can be obtained by expansions of functions, we get

$$\Lambda_h(v) = \lambda_h(v) + \mathcal{O}(h^2) \tag{4.1a}$$
$$= \lambda_h(v) + \mathcal{O}((h/\tau)^2). \tag{4.1b}$$

Equation (4.1b) indicates the similarity of $\Lambda_h(v)$ and $\lambda_h(v)$ when $h \ll \tau$, viz., unit time step is very small than the temperature-control parameter (see Appendix A for more detailed comparisons). Thus, the factor $\lambda_h(v)$, which was originally introduced in the Method 1 [20], can also be derived as an approximation of the factor $\Lambda_h(v)$ that appears as a component of $\Phi_h^{[3]}$ [equation (3.24c)], which is the exact flow of the decomposed Berendsen field, $X'^{[3]}$ [equation (3.20c)], which can also be identified with $X^{[3]}$, as stated. In other words, $\Lambda_h(v)$ is very natural for the original Berendsen EOM.

Equation (4.1) implies that the conventional methods can be seen as certain approximations, with respect to h, to the current method. To clarify this, first notice, as implied from (4.1a) (see Appendix B), the fact that

$$\Phi_h^{[3]}(\omega') = \tilde{\Phi}_h^{[3]}(\omega') + \mathcal{O}(h^2) \tag{4.2}$$

where

$$\tilde{\Phi}_h^{[3]}(\omega') \equiv (x,\, \lambda_h(v)v,\, \mathrm{v})\,. \tag{4.3}$$

Using these terminologies, we can redefine the conventional integrators as maps, constructed by $\tilde{\Phi}_h^{[3]}$ and a related one, on the extended space. First, Method 2 [equation (2.4)] can be represented as

$$\Phi_{\mathrm{M2},h} \equiv \Phi_h^{[4]} \circ \tilde{\Phi}_h^{[3]} \circ \Phi_{h/2}^{[2]} \circ \Phi_h^{[1]} \circ \Phi_{h/2}^{[2]}. \tag{4.4}$$

If we ignore the extended variable v, then (4.4) is completely consistent with (2.4). Here, v does not affect, as well as the original EOM, the development of x and v defined by the original Method 2, and v is changed (boosted) only by $\Phi_h^{[4]}$. Thus, $\Phi_h^{[4]}$ can be freely composed and we may define e.g., $\Phi_{\mathrm{M2},h} \equiv \tilde{\Phi}_h^{[3]} \circ \Phi_{h/2}^{[2]} \circ \Phi_h^{[1]} \circ \Phi_{h/2}^{[2]} \circ \Phi_h^{[4]}$ instead. The reason why we choose (4.4) is that we can take a similar form as our basic first-order map (3.26) [viz., $\Phi_h^{[4]}$ is placed at the last] to conduct their comparisons. This choice will also apply to other maps described below.

Similarly, Method 1 mod can be represented as

$$\Phi_{\mathrm{M1m},h} \equiv \Phi_h^{[4]} \circ \Phi_h^{[1]} \circ \tilde{\Phi}_h^{[3]} \circ \Phi_h^{[2]}. \tag{4.5}$$

Recall that Method 1 mod is a modification of Method 1 [equation (2.2)], which can now be represented by

$$\Phi_{\mathrm{M1},h} \equiv \Phi_h^{[4]} \circ \Phi_h^{[1]} \circ \check{\Phi}_h^{[3]} \circ \Phi_h^{[2]}, \tag{4.6}$$

where

$$\check{\Phi}_h^{[3]}(\omega') \equiv \left(x,\, \lambda_h(v - hF(x)\mathbf{M}^{-1})\, v,\, \mathrm{v}\right). \tag{4.7}$$

$\check{\Phi}_h^{[3]}$ is similar to $\tilde{\Phi}_h^{[3]}$ but not equivalent, and reflects the fact that in Method 1 the velocity before the mapping by $\Phi_h^{[2]}$ is referred as an argument of λ_h. Note that we have included $\Phi_t^{[4]}$ in $\Phi_{\mathrm{M1m},h}$ and $\Phi_{\mathrm{M1},h}$ using the same concept as that in $\Phi_{\mathrm{M2},h}$.

4.2. Similarity. Now, we can show, as detailed in Appendix B, that these three maps, $\Phi_{\mathrm{M1m},h}$, $\Phi_{\mathrm{M1},h}$, and $\Phi_{\mathrm{M2},h}$, are equivalent to Φ_h in the first-order accuracy, where Φ_h is a currently given map defined by (3.26). Namely,

$$\begin{aligned}\Phi_{\mathrm{M1m},h}(\omega') &= \Phi_h(\omega') + \mathcal{O}(h^2) \qquad (4.8)\\ &= \left(\Phi_h^{[4]} \circ \Phi_h^{[3]} \circ \Phi_h^{[2]} \circ \Phi_h^{[1]}\right)(\omega') + \mathcal{O}(h^2),\\ \Phi_{\mathrm{M1},h}(\omega') &= \Phi_h(\omega') + \mathcal{O}(h^2), \qquad (4.9)\\ \Phi_{\mathrm{M2},h}(\omega') &= \Phi_h(\omega') + \mathcal{O}(h^2). \qquad (4.10)\end{aligned}$$

As an intermediate type between $\Phi_{\mathrm{M1m},h}$ and Φ_h, a map,

$$\tilde{\Phi}_h \equiv \Phi_h^{[4]} \circ \tilde{\Phi}_h^{[3]} \circ \Phi_h^{[2]} \circ \Phi_h^{[1]}, \tag{4.11}$$

which uses $\tilde{\Phi}_h^{[3]}$ instead of $\Phi_h^{[3]}$ in Φ_h, can be defined and is also equivalent to Φ_h in the first order:

$$\tilde{\Phi}_h(\omega') = \Phi_h(\omega') + \mathcal{O}(h^2). \tag{4.12}$$

Since Φ_h is a first-order map, the above four maps become first-order integrators. Note that, however, this does not straightforwardly indicate that the maps do not have higher-order property. In particular, $\Phi_{\mathrm{M2},h}$ includes the part, $\Phi_{h/2}^{[2]} \circ \Phi_h^{[1]} \circ \Phi_{h/2}^{[2]}$, which corresponds to the second-order map for the Newtonian EOM, so that $\Phi_{\mathrm{M2},h}$ may behave as a second-order map if the Newtonian parts are dominant, as will be discussed later.

Computational cost of the current first-order map Φ_h and that of the conventional maps are essentially the same. In addition, the difference in the cost of between the current second-order P2S1 map [see (3.29) or (3.31)] and the conventional maps is at least $\mathcal{O}(n)$, which can be mostly ignored against the $\mathcal{O}(n^2)$-cost generally required in the force evaluation for $\Phi_h^{[2]}$. This is the consequence of the choice of the appearance ordering of $\Phi_h^{[j]}$, as discussed. However, note also that the cost becomes higher if use higher-order integrators, in general.

4.3. Difference. As stated, the conventional integrators, including the Berendsen's map $\Phi_{\mathrm{M1},h}$ and the related map $\Phi_{\mathrm{M1m},h}$, are equivalent to the current 1st-order scheme Φ_h in the lowest-order local accuracy. However, the current whole algorithm (3.32), using Φ_h and Φ_h^*, is not the same as the conventional methods, so that the overall behavior should not also be the same. The following three differences are given:

(i) Order of the local accuracy–. Equation (3.32) is at least the second order (which is the same as that of the Verlet method), while the conventional ones, $\Phi_{\mathrm{M1},h}$ and $\Phi_{\mathrm{M1m},h}$, are 1st order. This difference holds even when the current algorithm (3.32) uses $\tilde{\Phi}_h^{[3]}$, instead of $\Phi_h^{[3]}$.

(ii) Time reversibility (symmetric property)–. Here, a map ϕ_h parametrized by a time parameter h is said to be time reversible (at h), if $\phi_{-h} \circ \phi_h$ is well defined and becomes the identity; namely, if we go forward and then back with h, then we get to the starting point. Note that this is a fundamental property of *all* solutions of arbitrary smooth ODEs, including the original Berendsen EOM (2.1). Time reversibility is often referred as a symmetric property (here, we define the latter as a slightly stronger property than the former): ϕ_h is said to be symmetric (at h), if ϕ_h^* exists and $\phi_h^* = \phi_h$. Since a numerical integrator mimics the exact solutions of the original ODE, it should be symmetric. We see that Ψ_h [equation (3.32)] is symmetric provided that the parameters obey (3.33). In contrast, the conventional ones, $\Phi_{\mathrm{M1},h}$, $\Phi_{\mathrm{M2},h}$, and $\Phi_{\mathrm{M1m},h}$, are not. Note also that $\Phi_h^{[i]}$ $(i = 1, ..., 4)$ used in the current integrator are symmetric (time reversible), but $\tilde{\Phi}_h^{[3]}$ used in conventional integrators is not in general (where the usual group property is lost).

(iii) Robustness–. $\lambda_h(v)$ and $\Lambda_h(v)$ fluctuate according to the change of the kinetic energy $K(v)$ during the simulation; they are decreasing with increasing $K(v)$ for $h > 0$. By the following two reasons, the method using $\Lambda_h(v)$ is more robust than the method using $\lambda_h(v)$ (mathematical details are shown in Appendix A). (1) First, the amplitude of $\lambda_h(v)$ is larger than that of $\Lambda_h(v)$ for any $K(v)$ and any $h > 0$. This indicates that we often have to treat significant changes for $\lambda_h(v)$ in general. Since this comparison is for the same $K(v)$ value but not for the same simulation step, the above indication makes sense as long as the dynamics obtained by using $\Lambda_h(v)$ encounters similar or smaller fluctuations of $K(v)$ than those obtained by using $\lambda_h(v)$. (2) Second, if we increase the value of h/τ, viz., increasing h and/or decreasing τ, then the difference of the two amplitudes, $|\lambda_h(v) - \Lambda_h(v)|$, becomes large. This indicates that the scheme using $\Lambda_h(v)$ becomes more robust than that using $\lambda_h(v)$, as we increase h to use a larger timestep and/or decrease τ to control the temperature faster. Here, note that the parameters τ and h/τ appear only in $\Phi_h^{[3]}$, $\tilde{\Phi}_h^{[3]}$, and $\check{\Phi}_h^{[3]}$, through $\lambda_h(v)$ and $\Lambda_h(v)$.

5. Numerical Simulation. Among the current integrators, we examined the most fundamental one, P2S1, in detail and compared it with the conventional methods, Method 1, Method 1 mod, and Method 2. A basic model system and two bulk systems were used for the examinations. All the simulations were performed with a program specially developed for this study.

5.1. Material. (1) Isolated ethane molecule. The molecule is designed by two CH_3 united atoms ($m_1 = m_2 = 15$ g/mol) and one harmonic spring connecting the two united atoms. The interaction is thus $U(r) = k(r - r_0)^2$, where r is the distance between the atoms, r_0 is its equilibrium value, and k is the spring constant. The parameters used were $r_0 = 1.54$ Å and $k = 240$ Å^{-2}kcal/mol, and the target temperature T_0 was 300 K, as set in [46]. The initial coordinates $x(0) \equiv (\boldsymbol{x}_1(0), \boldsymbol{x}_2(0))$ and velocities $v(0) \equiv (\boldsymbol{v}_1(0), \boldsymbol{v}_2(0))$ were $\boldsymbol{x}_1(0) = -\boldsymbol{x}_2(0) = (-0.8, 0, 0)$ and $\boldsymbol{v}_1(0) = -\boldsymbol{v}_2(0) = (\sigma, 0, 0)$, where $\sigma = \sqrt{3k_{\mathrm{B}}T_0/m_1}$. With these settings, the total linear and angular momenta are initially zero, and the temperature is initially the target temperature. The initial value of the extended variable was set to $\mathrm{v}(0) = 0$.

(2) Bulk argon system. The interactions of argon atoms are defined by a pairwise

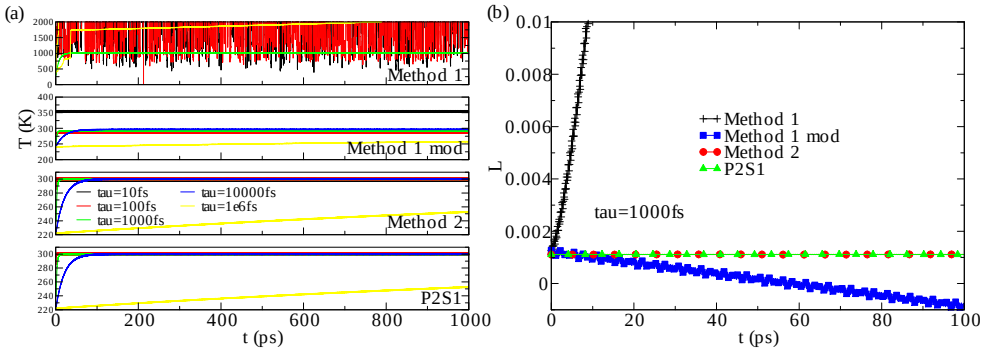

FIG. 5.1. *(a) Trajectories of averaged temperature, $T_{\rm MA}$, for a single ethane molecule system obtained by four integration methods: Method 1, Method 1 mod, Method 2, and P2S1. Temperature-control time constant τ is varied, while the unit timestep h is 1 fs. (b) Trajectories of the invariant function L ($Å^2$ g/mol fs^{-2}) using the four methods with $h = 1$ fs and $\tau = 1$ ps.*

Lennard-Jones type potential with the smooth force-switching scheme of the form,

$$U(r) = \begin{cases} Ar^{-12} - Br^{-6} + a_0 & \text{for} \quad 0 < r \le r_1, \\ a_0 + \sum_{k=0}^{4} b_k r^k & \text{for} \quad r_1 < r < r_{\rm c}, \\ 0 & \text{for} \quad r_{\rm c} \le r < \infty, \end{cases} \tag{5.1}$$

where $A = 2508000$ Å^{12}kcal/mol and $B = 1545$ Å^{6}kcal/mol. The original force function is defined for $r \le r_1$ and it is smoothly damped zero at the cutoff length $r_{\rm c}$, where $r_1 = 8$ Å and $r_{\rm c} = 10$ Å were used. The parameters, a_k and b_k, are determined so as to U be a smooth function, e.g., $a_0 = -\sum_{k=0}^{4} b_k r_{\rm c}^k$ (see [42] for the details). 168 argon atoms were treated within a $20 \times 20 \times 20$ Å^3 cubic box under the 3D periodic boundary condition. The target temperature T_0 was 87 K, which corresponds to a liquid phase. The initial velocities were set randomly, modified to zero the total linear momentum, and scaled to obtain an initial kinetic energy equal to the target kinetic energy. The initial value of the extended variable was set to $v(0) = 0$.

(3) Bulk ethane system. The intramolecular interaction is the same as that in (1), and the intermolecular interactions were defined by a pairwise potential of the same form as (5.1) with $A = 6020089$ Å^{12}kcal/mol, $B = 2165$ Å^{6}kcal/mol [47], $r_1 = 12$ Å, and $r_{\rm c} = 14$ Å. 588 molecules were treated within a $30 \times 30 \times 30$ Å^3 cubic box under the 3D periodic boundary condition. T_0 was 184 K. The initial velocities were set randomly, modified to zero the total linear momentum, and scaled to obtain an initial kinetic energy equal to the target value. The extended variable was set to $v(0) = 0$.

5.2. Results and discussion.

5.2.1. Isolated molecule. To investigate fundamental properties of the integrators, we first apply them to a simple model system, an isolated ethane molecule. We have studied the following four properties: (i) temperature control ability, (ii) accuracy, (iii) robustness, and (iv) time reversibility.

(i) Since this system is small, the temperature fluctuations should be large so that the temperature control will not be trivial. To see this, we have varied the value of the temperature-control time constant τ. Here, in general, a small τ increases the temperature controlling speed but introduces stiffness in the system. In contrast, a large τ decreases the controlling speed and results in no temperature control in

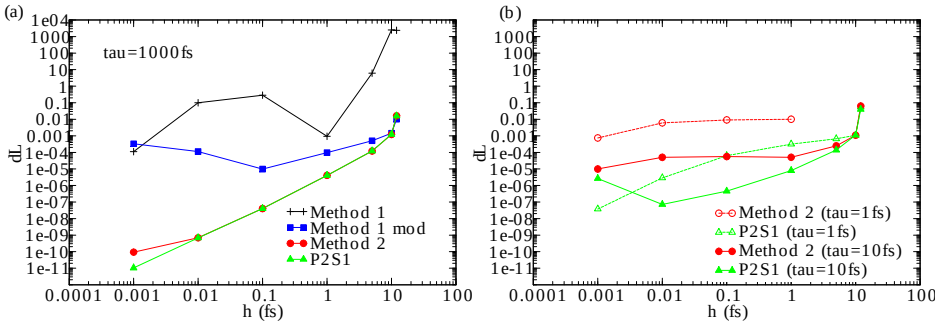

FIG. 5.2. *The errors of the invariant function obtained for the single ethane molecule system. Unit timestep h is varied. (a) Four integration methods using* $\tau = 1000$ *fs. (b) Method 2 and P2S1 using* $\tau = 1$ *or* 10 *fs.*

the Newtonian limit $\tau \to \infty$. Figure 5.1(a) shows averaged time development of the temperature obtained by the four integration methods using $h = 1$ fs and several τ values. Here, to properly capture the control ability, simple moving average, $T_{\rm MA}(n) \equiv \frac{1}{N_{\rm MA}} \sum_{i=1}^{N_{\rm MA}} T(n-i+1)$, is depicted for $n \geq N_{\rm MA} \equiv 1000$, instead of the instantaneous temperature at time $t = nh$, $T(n)$ (see Figure S1 in Supplementary materials for the instantaneous temperature). Method 1 was not satisfactory for this system. For smaller τ, the fluctuations are enormously large, relative to the target temperature T_0, and for larger τ the fluctuations are smaller but the averaged temperature is too high compared with T_0. Method 1 mod was better than Method 1, suggesting that the velocity scaling using the boosted velocity $\tilde{v} = v + hF(x)\mathbf{M}^{-1}$ is better than using the original velocity v [viz., $\lambda_h(\tilde{v})\tilde{v}$ was better than $\lambda_h(v)\tilde{v}$ in (2.2)]. However, the averaged temperatures of Method 1 mod are still far from T_0 for the largest and smallest τ. Method 2 and P2S1 are comparable, and the temperature control is good except for the largest τ. The smaller the τ the faster the control becomes, as theoretically expected, and it does work even for the smallest τ.

(ii) We have checked the numerical error by the conservation of the invariant function defined by (3.16) applying (3.14). Figure 5.1(b) shows the trajectory of the invariant (Å^2 g/mol fs^{-2}) obtained by each method with $h = 1$ fs and $\tau = 1$ ps. The drift in Method 1 is significant, which may be expected from the temperature controllability as discussed above. Method 1 mod also exhibits unignorable drift, although the temperature control is relatively good for these h and τ values as shown in Figure 5.1(a). This indicates that the judgement of the simulation validity only by the temperature controllability is in fact insufficient. Method 2 and P2S1 are comparable and show good conservations of the invariant.

To investigate the accuracy in detail, the global error was estimated by the error of the invariant dL, which was obtained by the following formula in order to properly capture the behavior of the trajectory of L, as described in [42]:

$$dL = \left\langle \langle |L(t) - L(t_0)| \rangle \Big|_{t=t_0}^{t_0+\mathrm{sd}} \right\rangle \Big|_{t_0}, \tag{5.2}$$

where one thousand different time origins, t_0, have been chosen randomly, and the sampling duration, sd, was 10 ps. Figure 5.2(a) shows the error dL measured with varying the unit time step h. Method 1 generates large errors especially for $h >$ 1 fs. Method 2 and P2S1 are comparable and imply good second-order integrator behavior [42]. Their difference is only in a very small h for $\tau = 1$ ps.

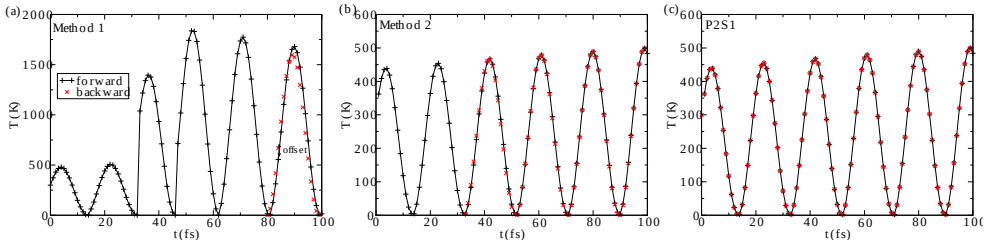

FIG. 5.3. *The reversibility for (a) Method 1, (b) Method 2, and (c) P2S1, tested on the single ethane molecule system. Black "+" designates the temperature of each timestep obtained in the forward simulation, while red "×" the backward simulation. "Offset" shows the deviation between the forward and backward values.*

The resemblance between Method 2 and P2S1 may imply a special relationship between them. Although Method 2 is not considered to be an exact second-order map, it may have a certain relation with the second-order P2S1 map Ψ_h^{P2S1}, in contrast to Method 1 and Method 1 mod. For example, under "mild" conditions such that $K(v) \sim K_0$ (near equilibrium) and/or $s \equiv h/\tau$ is sufficiently small (non "stiff"), it may hold that $\Phi_{\mathrm{M2},h} \sim \Psi_h^{\mathrm{P2S1}} + \mathcal{O}(s^3)$ or a weaker relationship such as $\Phi_{\mathrm{M2},h} \sim \varphi_h \circ \Psi_h^{\mathrm{P2S1}} \circ \varphi_h^{-1} + \mathcal{O}(s^3)$ for a certain invertible map φ_h (viz., φ_h becomes a postprocessor [48] between Ψ_h^{P2S1} and $\Phi_{\mathrm{M2},h}$ in an approximate sense). These relationships suggest a second-order like property for $\Phi_{\mathrm{M2},h}$.

(iii) Robustness of the current method in the sense of (iii-1) demonstrated in section 4.3 should be already clear from the simulation difference to the conventional methods, Method 1 and Method 1 mod, shown above. The indication on issue (iii-1) in section 4.3 really makes sense, because the dynamics generated by P2S1 using $\Lambda_h(v)$ encounter similar or smaller fluctuations of $K(v)$ than the dynamics generated by Method 1, Method 1 mod, and Method 2, all of which use $\lambda_h(v)$.

The robustness of P2S1 in the sense of (iii-2) in section 4.3, originated from the difference between $\lambda_h(v)$ and $\Lambda_h(v)$ [viz., the difference between $\tilde{\Phi}_h^{[3]}$ and $\Phi_h^{[3]}$], will be clearer by increasing $s \equiv h/\tau$. This also reveals the difference between Method 2 and P2S1, as depicted in Figure 5.2(b), which shows dL measured using τ that is smaller than in Figure 5.2(a). For $\tau = 10$ fs, the accuracy of P2S1 is superior than Method 2 with the order from one to two for $h \leq 1$ fs, although the difference vanishes for a larger h because the principal error may come from the common maps $\Phi_h^{[2]}$ and $\Phi_h^{[1]}$. For $\tau = 1$ fs, the difference between Method 2 and P2S1 is clearer, and Method 2 broke for $h > 1$ fs, due to the domain exception problem (see Appendix A for details).

(iv) Figure 5.3 shows the results of a time reversing test. After a "forward" simulation for $M = 100$ time steps with unit time step $h = 1$ fs, it was changed into the negative value, viz., $h = -1$ fs, and a "backward" simulation was conducted for M time steps. If the trajectory is exact, then we will have the same (x, v) value at $M-m$ time step and at $M+m$ time step for every $m = 1, .., M$. They were deviated much for Method 1, as indicated in Figure 5.3(a). Furthermore, it broke at $M+21$ time step due to the use of negative time step (see Appendix A). For Method 2 [Figure 5.3(b)], the correspondence between $M-m$ and $M+m$ is better, but the deviations were gradually increased and also resulted in a break at $M+67$ steps. In contrast, the correspondence is almost perfect for P2S1 and resulted in the same (x, v) value at the final $2M$ time steps as the initial value [Figure 5.3(c)]. These results clearly indicate that the current P2S1 method is really time reversible, which is a fundamental property of the

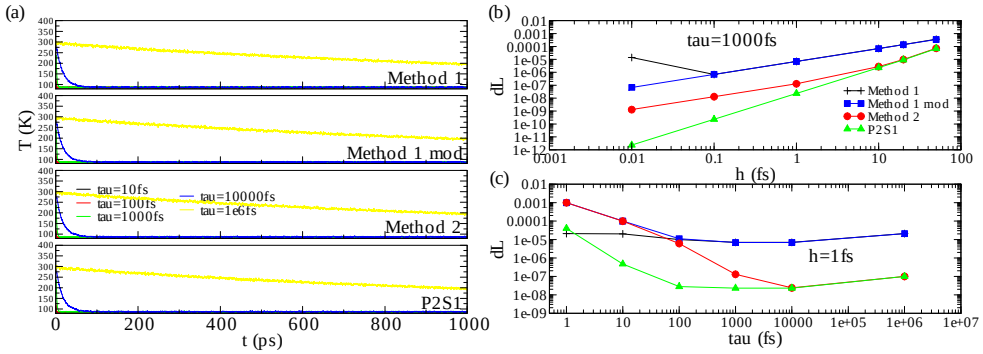

FIG. 5.4. *(a) Trajectories of the averaged temperature for a bulk argon system obtained by Method 1, Method 1 mod, Method 2, and P2S1. Temperature-control time constant τ is varied. The errors of the invariant function are shown with (b) unit timestep h being varied (abscissa) with τ fixed to be 1 ps, and (c) τ being varied (abscissa) with h fixed to be 1 fs.*

original ODE and should be possessed by accurate numerical integrators. Note that "backward" simulation is not done in ordinary simulations, but it is preferable to have many measures, including the "backward" simulation analysis, to detect numerical errors, where the loss of the time reversibility indicates potential errors.

5.2.2. Bulk argon. Figure 5.4(a) shows the trajectories of averaged temperature T_{MA} in the bulk argon system using $h = 1$ fs. Temperature control ability resembled for all the methods, for which a smaller τ conducts quick control and a larger τ leads to slow control, as expected. This resemblance is in contrast to the smaller system, the isolated molecule, discussed above. However, the accuracy measured by the invariant deviation dL clarified the difference between the methods. Figure 5.4(b) shows dL, which was estimated in the same manner as the isolated molecule system, by using several h values and a fixed τ value at 1 ps. The accuracies of P2S1 and Method 2 are one or two orders of magnitude better than that of Method 1 and Method 1 mod for a wide range of h. The difference between P2S1 and Method 2 is larger for a smaller h and it vanishes for practical h values. However, the difference becomes large for a smaller τ, as shown in Figure 5.4(c), where dL was estimated using several τ values and a fixed h value at 1 fs. The difference between P2S1 and Method 2 is one or two order of magnitude for $\tau \lesssim 1000$ fs. This clearly shows the robustness of the current method, which thus enables quick and accurate temperature control using a small τ.

5.2.3. Bulk ethane. The robustness of the current method was also observed in the bulk ethane system, as shown in Figure 5.5. For $\tau = 1$ ps, the accuracies of the two methods, P2S1 and Method 2, are one or more orders of magnitude better than that of the remaining two methods, Method 1 and Method 1 mod. However, for $\tau = 10$ fs, the situation clearly changed, and only P2S1 is accurate, with two or more orders of magnitude, compared with Method 1, Method 1 mod, and Method 2 for a wide range of h. The maximum h value for P2S1 with the $\tau = 10$ fs case was 11 fs.

Remarks regarding the dL vs. h curves are made. These curves are very smoother than those obtained in the single molecule system indicated in Figure 5.2(a). This should be related to the fact that the temperature deviation of the small system is large (see Figure S1 in Supplementary materials) so that the temperature control is difficult, resulting in a stiffness to the system. On the other hand, the gradient of the curve

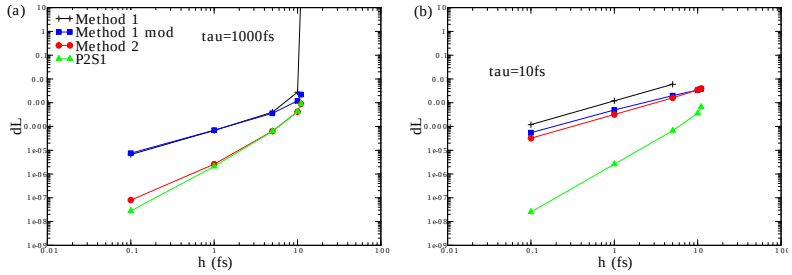

FIG. 5.5. *The errors of the invariant function obtained for a bulk ethane system using the four integration methods. Unit time step* h *is varied with* τ *fixed to be (a)* 1 *ps and (b)* 10 *fs.*

is considered to correspond the local order of the accuracy [42]. In this viewpoint, Method 2 seems to be a second-order integrator if $\tau = 1000$ fs [Figure 5.5(a)] but it seems to be a first-order integrator if $\tau = 10$ fs [Figure 5.5(b)]. Thus, Method 2 is implied to have a intermediate property between these two accuracies.

6. Conclusion. The proposed scheme for numerically integrating the Berendsen temperature-control EOM works well in respect of the temperature-control ability, accuracy, robustness, and time reversibility. It was analyzed theoretically and examined numerically by simulating an isolated ethane molecule, a bulk argon system, and a bulk ethane system.

The superiority of the proposed integrator in the temperature-control ability is clear in a stiff system, which is here an isolated molecule system having larger fluctuations. The proposed P2S1 integrator and the conventional integrators are equivalent in the computational cost and the first-order local accuracy. But P2S1 is second order, and also the proposed scheme enables us to attain a higher accuracy. The accuracy measured by the invariant function for P2S1 was one or two orders of magnitude better than that of the conventional integrators, for a wide range of h and in particular for a small τ, where h is the unit time step and τ is the temperature-control time constant of the EOM. The robustness of the proposed method is also clear if we use a larger ratio, h/τ. It thus allows to use, as well as a large h, a small τ, which leads to a subtle control of the temperature of the physical system. The robustness of the proposed method comes from the velocity scale factor $\Lambda_h(v)$, which is a counterpart of $\lambda_h(v)$ used in conventional methods. Although a suitable τ value may depend on physical consideration or simulation purpose, the results provided by the proposed method were similar or superior than those of the conventional methods for all τ values investigated. The proposed operator-map scheme is successful to capture the property of the original ODE, the time reversibility. The time reversibility of the proposed method comes from a suitable decomposition of the Berendsen vector field and the symmetric composition technique of the resultant exact maps.

In this study, we restrict our attention on the most fundamental scheme, P2S1, among the proposed methods. This is because it is simply implemented while highly effective. Higher-order integration schemes, such as fourth-order integrators P4S5 and P4S6, can be used according to the proposed method, in order to attain higher accuracy for a small h. For a larger h, an alternative second-order integrator, P2S2, is useful and will show a comparable or better performance relative to P2S1. In this study, as the basis for these comparisons, P2S1 was shown to be better than the conventional schemes by the numerical simulations.

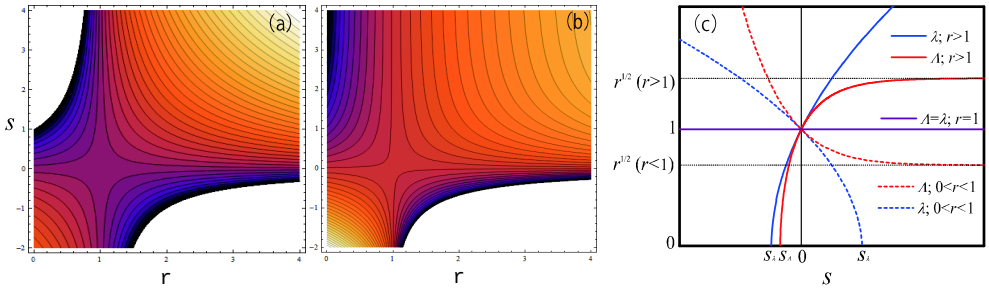

FIG. 7.1. *Velocity scale factors* $\lambda(r,s) = [1 + s\,(r-1)]^{\frac{1}{2}}$ *and* $\Lambda(r,s) = [(1-r)\exp(-s) + r]^{\frac{1}{2}}$, *where* $r \equiv K_0/K(v)$ *and* $s \equiv h/\tau$. *Domains of definition of (a)* λ *and (b)* Λ *are shown, as well as contours (large as light color). (c) Values of the factors with respect to* s, *where* $r \equiv 2 > 1$, $r \equiv 1$, *and* $r \equiv 0.5 < 1$ *cases are indicated.*

We also showed that a good performance of the numerical integrator was not measured by only the temperature-control ability. The currently proposed invariant function defined on the extended phase space is useful for any integrator to catch the numerical error and to prevent unphysical results.

7. Appendix A. Here we analyze and compare the two velocity scale factors: conventional one, $\lambda_h(v)$, and the currently introduced one, $\Lambda_h(v)$.

7.1. Basics. To simplify the discussion, we re-parametrize these factors, using $s \equiv h/\tau \in \mathbb{R}$ (the ratio of a unit time step to the time constant) and $r \equiv K_0/K(v) \in \mathbb{R}_+$ (the ratio of the target value to a variable for the kinetic energy; $\mathbb{R}_+$ denotes strictly positive numbers), such that

$$\lambda(r,s) = [1 + s\,(r-1)]^{\frac{1}{2}}\,, \tag{7.1}$$

$$\Lambda(r,s) = [(1-r)\exp(-s) + r]^{\frac{1}{2}}\,, \tag{7.2}$$

reducing $\lambda(K_0/K(v), h/\tau) = \lambda_h(v)$ and $\Lambda(K_0/K(v), h/\tau) = \Lambda_h(v)$. Since we need real-valued factors, first we should clarify the domain of definition of λ and that of Λ. They are, respectively, given by

$$\Gamma_\lambda \equiv \{(r,s) \in \mathbb{R}_+ \times \mathbb{R} |\ s \le s_\lambda(r) \text{ if } r < 1, \text{ and } s \ge s_\lambda(r) \text{ if } r > 1\}, \tag{7.3}$$

$$\Gamma_\Lambda \equiv \{(r,s) \in \mathbb{R}_+ \times \mathbb{R} |\ s \ge s_\Lambda(r) \text{ if } r > 1\} \tag{7.4}$$

[see Figures 7.1 (a) and (b)], where

$$s_\lambda(r) \equiv (1-r)^{-1}, \tag{7.5a}$$

$$s_\Lambda(r) \equiv \ln(1 - r^{-1}). \tag{7.5b}$$

7.1.1. Domain exception problem. The integrator breaks down if λor Λ takes a value out of Γ_λ or Γ_Λ.

($r = 1$ *case*) Since

$$\lambda(1,s) = \Lambda(1,s) = 1 \tag{7.6}$$

holds for all $s \in \mathbb{R}$, there is no problem in this case, as expected from the fact that $r = 1$ means the "equilibrium" $K_0 = K(v)$.

($r < 1$ *case*) If $r < 1$, then admissible s for $\lambda(r, s)$ is restricted such that $s \le s_\lambda(r)$, but this condition is met as long as $s \le 1$, namely, $h \le \tau$. Thus, the domain exception problem may not be severe in many practical simulations (nevertheless, we have confirmed this problem for Method 2 in Figure 5.2(b)). In contrast, since all $s \in \mathbb{R}$ is admissible for $\Lambda(r, s)$ when $r < 1$, no problem arrises in the proposed method.

($r > 1$ *case*) If $r > 1$, then every $s \ge 0$ is admissible for both λ and Λ [since $s_\lambda(r), s_\Lambda(r) < 0$ if $r > 1$], while the use of negative s is restricted. We have encountered this type of domain exception in the backward simulation for the conventional methods as seen in Figures 5.3(a) and 5.3(b). In contrast, for the current method using Λ in $\Phi_h^{[3]}$, the usual group property, $(\Phi_{-h}^{[3]} \circ \Phi_h^{[3]})(\omega') = \omega'$, ensures no exception in the backward simulation. However, this type of the domain exception concerns higher-order integrators (see section 7.3).

7.1.2. Graph. Both λ and Λ are monotonic functions with respect to both r and s (strictly monotonic unless $r = 1$ or $s = 0$). Typical graphs are depicted in Figure 7.1(c). Equation (4.1) can be obtained (see also Remark 8.6 in Appendix B) from the Maclaurin's expansion of λ and Λ with respect to s such that

$$\Lambda(r, s) = 1 + \frac{1}{2}(r - 1)s - \frac{1}{8}(r^2 - 1)s^2 + \mathcal{O}(s^3), \tag{7.7a}$$

$$\lambda(r, s) = 1 + \frac{1}{2}(r - 1)s - \frac{1}{8}(r - 1)^2 s^2 + \mathcal{O}(s^3). \tag{7.7b}$$

Note that $\Lambda(r, s) \ne \lambda(r, s) + \mathcal{O}(s^3)$ in general (the equality holds only in the "equilibrium" case $r = 1$).

7.2. The statements on the robustness. We mathematically formulate the statements on issues (iii-1) and (iii-2) in section 4.3 as Propositions 7.2 and 7.3, respectively. Proofs of propositions are given in section III of Supplementary materials.

Issue (iii-1). When $r = 1$, viz., kinetic energy $K(v)$ takes the target value K_0, then the factors do nothing, that is, (7.6) holds. In simulations, r varies so that λ and Λ fluctuate around the unity. As a fundamental property, we observe

PROPOSITION 7.1. *(a) If* $0 < r < 1$ *then* $\lambda(r, s) = \Lambda(r, s) = 1$ *for* $s = 0$ *and* $\lambda(r, s) < \Lambda(r, s)$ *for all admissible* $s \ne 0$*, (b) if* $r = 1$ *then* $\lambda(r, s) = \Lambda(r, s) = 1$ *for all* $s \in \mathbb{R}$*, and (c) if* $r > 1$ *then* $\lambda(r, s) = \Lambda(r, s) = 1$ *for* $s = 0$ *and* $\lambda(r, s) > \Lambda(r, s)$ *for all admissible* $s \ne 0$*.*

Now, we see that the amplitude of $\lambda(r, s)$ from its "equilibrium" value 1 is larger than that of $\Lambda(r, s)$:

PROPOSITION 7.2. $|\lambda(r, s) - 1| \geqq |\Lambda(r, s) - 1|$ *holds for any* $(r, s) \in \Gamma_\lambda \cap \Gamma_\Lambda$ *provided that* $s > 0$*, where the equality holds only if* $r = 1$*.*

Issue (iii-2). Consider the behavior of $\lambda(r, s)$ and $\Lambda(r, s)$ as increasing $s = h/\tau$, viz., increasing the unit time step h or decreasing the temperature-control time constant τ. As for a global behavior, $\Lambda(r, s)$ is bounded for $s \ge 0$ and $\lim_{s\to\infty} \Lambda(r, s) = r^{\frac{1}{2}}$ for any $r > 0$, but $\lambda(r, s)$ is not. In fact, $\lim_{s\to\infty} \lambda(r, s) = \infty$ if $r > 1$, and $\lambda(r, s)$ cannot be defined anymore for $s > s_\lambda(r)$ if $r < 1$. This implies that $\lambda(r, s)$ is not tractable for increasing s. These differences of the global behavior between $\lambda(r, s)$ and $\Lambda(r, s)$ are in contrast to the similarities of the local behavior between them, as seen in (7.7). The importance in practice may be in the middle range of s. As expected from these facts, the behavior of the difference between $\lambda(r, s)$ and $\Lambda(r, s)$ is described as follows, which now expresses the statement in (iii-2):

PROPOSITION 7.3. *$|\lambda(r,s)-\Lambda(r,s)|$ is strictly monotone increasing with respect to s for any admissible $s>0$ and for an arbitrarily fixed $r\in\mathbb{R}_+\backslash\{1\}$.*

7.3. Robust higher-order method. For constructing a robust higher-order integration method, we should overcome the problem originated from the fact that $\Lambda_h(v)$ does not permit an arbitrary $h\in\mathbb{R}$. Namely, the domain of the definition of $\Lambda(r,s)$ for a fixed r is $[s_\Lambda(r),\infty)\subsetneqq\mathbb{R}$ if $r>1$, while it is whole $\mathbb{R}$ if $0<r\le 1$. From this fact, one cannot use arbitrary *negative* coefficients $\{\alpha_i,\beta_i\}$ in (3.32), since $\alpha_i h$ and $\beta_i h$ play a role of an intermediate unit timestep and require the evaluation of $\Lambda_{\alpha_i h}(v)$ and $\Lambda_{\beta_i h}(v)$. One way to solve this problem is to use a higher-order integrator whose coefficients are all positive [49, 50, 51]. The other way is to use, instead of $\Lambda(r,s)$, its suitable approximation, $\hat\Lambda(r,s)$, which is defined for all $h\in\mathbb{R}$ to enable us to use any negative coefficients. The map $\hat\Phi_h^{[3]}$, which uses $\hat\Lambda$ instead of Λ, should also be 1-1 for all h, in order to construct its adjoint map.

8. Appendix B: Proof of the first-order accuracy. We prove the formulas, (4.8)–(4.10) and (4.12), which demonstrate the similarities of the integrators in the sense that they are all equivalent within the first-order accuracy. We also reconsider (4.1) and (4.2). Before proving the formulas, we state our notations and assumptions.

Notation: For simplicity, the extended phase space Ω' shall be written by Ω, so that $\Omega\equiv D\times\mathbb{R}^n_\times\times\mathbb{R}$, where D is a domain of $\mathbb{R}^n$ and $\mathbb{R}^n_\times\equiv\mathbb{R}^n\backslash\{0\}$, and the phase-space point is denoted as $\omega=(x,\,v,\mathrm{v})\in\Omega$. For convenience, we use the notation such that $\Phi_h^{[\tilde 3]}\equiv\tilde\Phi_h^{[3]}$ and $\Phi_h^{[\check 3]}\equiv\check\Phi_h^{[3]}$, so that all the maps, $\Phi_h^{[1]}$, $\Phi_h^{[2]}$, $\Phi_h^{[3]}$, $\Phi_h^{[4]}$, $\tilde\Phi_h^{[3]}$, and $\check\Phi_h^{[3]}$, can be represented uniformly as $\Phi_h^{[i]}$ with $i\in B\equiv\{1,2,3,4,\tilde 3,\check 3\}$. According to each consideration, we often denote $\Phi_h^{[i]}(\omega)$, where $\omega\in\Omega$ is treated to be a variable and $h\in\mathbb{R}$ be a parameter, by $\Phi^{[i]}(\omega,h)$, which treats both ω and h to be variables, or by $\Phi^{[i]\omega}(h)$, which treats h to be a variable and ω be a parameter.

Assumption: We assume that the functions, the force function $F:D\to\mathbb{R}^n$ and the extended-field function $Y:D\times\mathbb{R}^n_\times\to\mathbb{R}$, are sufficiently smooth (e.g., twice differentiable). The kinetic-energy function $K:\mathbb{R}^n_\times\to\mathbb{R}_+$ should also be smooth [it does not necessarily takes the form of $K(v)\equiv\sum_{i=1}^n m_i v_i^2/2$ but takes values in $\mathbb{R}_+$, viz., strictly positive, for $v\neq 0$].

8.1. Basics. We should consider two technical points. First, we should clarify the admissible range for the unit time step, h. This problem arises in $\Phi_h^{[i]}$ for $i\in\{3,\tilde 3,\check 3\}$, originated from the well-definedness of $\Lambda_h(v)$ and $\lambda_h(v)$ discussed in Appendix A. The second point is that each $\Phi_h^{[i]}$ should map any phase-space point $\omega=(x,\,v,\mathrm{v})$ in Ω to $\omega'=(x',\,v',\mathrm{v}')$ that is also in Ω, meaning that we should ensure $x'\in D$ and $v'\neq 0$. This is required to consider the composition of these mappings, because the maps $\Phi_h^{[i]}$ are not defined outside Ω. The second point concerns with all the maps $\Phi_h^{[i]}$ ($i\in B$), and in fact it turns out to be a condition on h as shown below. Thus the second point is relevant to the first point. Hence, what we should clarify is the range of h in which $\Phi_h^{[i]}(\omega)$ is well defined [i.e., $(\omega,h)\in\Omega^{[i]}$; see below] and takes a value in Ω [i.e., $\Phi^{[i]}(\omega,h)\in\Omega$; see below].

To handle these points, at first, we mainly treat the maps by explicitly considering h-dependence as $\Phi^{[i]}(\omega,h)$: $\Phi^{[i]}$ is a map from a certain subset of $\Omega\times\mathbb{R}$ into $\mathbb{R}^{2n+1}$,

$$\Phi^{[i]}:\Omega\times\mathbb{R}\supset\Omega^{[i]}\to\mathbb{R}^{2n+1},\ (\omega,h)\mapsto\Phi_h^{[i]}(\omega),\tag{8.1}$$

for $i \in B$, and individually described as follows:

$$\begin{aligned}
&\Phi^{[1]} : \Omega^{[1]} \to \mathbb{R}^{2n+1},\ (\omega, h) \mapsto (hv + x,\ v, \mathrm{v}),\\
&\Phi^{[2]} : \Omega^{[2]} \to \mathbb{R}^{2n+1},\ (\omega, h) \mapsto \left(x,\ hF(x)\mathbf{M}^{-1} + v,\ \mathrm{v}\right),\\
&\Phi^{[4]} : \Omega^{[4]} \to \mathbb{R}^{2n+1},\ (\omega, h) \mapsto (x,\ v,\ hY(x, v) + \mathrm{v}),\\
&\Phi^{[3]} : \Omega^{[3]} \to \mathbb{R}^{2n+1},\ (\omega, h) \mapsto (x,\ \Lambda_h(v)v,\ \mathrm{v}),\\
&\Phi_h^{[\tilde{3}]} : \Omega^{[\tilde{3}]} \to \mathbb{R}^{2n+1},\ (\omega, h) \mapsto (x,\ \lambda_h(v)v,\ \mathrm{v}),\\
&\Phi^{[\check{3}]} : \Omega^{[\check{3}]} \to \mathbb{R}^{2n+1},\ (\omega, h) \mapsto \left(x,\ \lambda_h(v - hF(x)\mathbf{M}^{-1})\, v,\ \mathrm{v}\right).
\end{aligned}$$

Here, $\Omega^{[i]}$ for $i \in \{1, 2, 4\}$ is simply defined by $\Omega^{[i]} := \Omega \times \mathbb{R}$, while $\Omega^{[3]}$ and $\Omega^{[\tilde{3}]}$ are defined, so that $\Lambda_h(v)$ and $\lambda_h(v)$ are well defined respectively, by

$$\Omega^{[3]} \ :=\ H^{-1}(\Gamma_\Lambda) \tag{8.2a}$$

$$=\ \{(x,\ v, \mathrm{v}, h) \in \Omega \times \mathbb{R} |\ h/\tau \geq s_\Lambda(K_0/K(v)) \text{ if } K_0 > K(v)\} \tag{8.2b}$$

and

$$\Omega^{[\tilde{3}]} \ :=\ H^{-1}(\Gamma_\lambda) \tag{8.3a}$$

$$=\ \left\{(x,\ v, \mathrm{v}, h) \in \Omega \times \mathbb{R} \ \middle|\ \begin{array}{lll} h/\tau \leq s_\lambda(K_0/K(v)) & \text{if} & K_0 < K(v), \\ h/\tau \geq s_\lambda(K_0/K(v)) & \text{if} & K_0 > K(v) \end{array} \right\}, \tag{8.3b}$$

where

$$H : \Omega \times \mathbb{R} \to \mathbb{R}^2, (x,\ v, \mathrm{v}, h) \overset{\mathrm{d}}{\mapsto} (K_0/K(v), h/\tau). \tag{8.4}$$

Similarly, $\Omega^{[\check{3}]}$ is defined by

$$\Omega^{[\check{3}]} \ :=\ \left(\bar{\Phi}^{[2-]}\right)^{-1}(\Omega^{[\tilde{3}]}) \tag{8.5a}$$

$$=\ \{(x,\ v, \mathrm{v}, h) \in \Omega \times \mathbb{R} |\ (x,\ v - hF(x)\mathbf{M}^{-1},\ \mathrm{v}, h) \in \Omega^{[\tilde{3}]}\}, \tag{8.5b}$$

where

$$\bar{\Phi}^{[2-]} : \Omega \times \mathbb{R} \to \mathbb{R}^{2n+1} \times \mathbb{R}, (\omega, h) \overset{\mathrm{d}}{\mapsto} (\Phi^{[2]}(\omega, -h), h) = (x,\ v - hF(x)\mathbf{M}^{-1},\ \mathrm{v}, h). \tag{8.6}$$

Thus we have prepared to state about the range of h and represent it as follows:

Proposition 8.1. *For each $i \in B$, $(\omega, h) \in \Omega^{[i]}$ and $\Phi^{[i]}(\omega, h) \in \Omega$ if and only if $(\omega, h) \in \left(\Phi^{[i]}\right)^{-1}(\Omega)$. Here, we have an explicit form as follows:*

$$\left(\Phi^{[i]}\right)^{-1}(\Omega) = \bigcup_{\omega = (x,\ v, \mathrm{v}) \in \Omega} \{\omega\} \times \mathring{I}^{[i]\omega} =: \Omega^{[i]\prime}, \tag{8.7}$$

where

$$\mathring{I}^{[i]\omega} := \left(\Phi^{[i]\omega}\right)^{-1}(\Omega) \text{ for } i \in \{1, 2, 4\}, \tag{8.8a}$$

$$\mathring{I}^{[3]\omega} := \begin{cases} (\tau\, s_\Lambda(K_0/K(v)),\ \infty) & \text{if} \quad K(v) < K_0, \\ \mathbb{R} & \text{if} \quad K(v) \geq K_0, \end{cases} \tag{8.8b}$$

$$\mathring{I}^{[\tilde{3}]\omega} := \begin{cases} (\tau\, s_\lambda(K_0/K(v)),\ \infty) & \text{if} \quad K(v) < K_0, \\ \mathbb{R} & \text{if} \quad K(v) = K_0, \\ (-\infty,\ \tau\, s_\lambda(K_0/K(v))) & \text{if} \quad K(v) > K_0, \end{cases} \tag{8.8c}$$

$$\mathring{I}^{[\check{3}]\omega} := \left(H \circ \left(\bar{\Phi}^{[2-]\omega} | U_\omega\right)\right)^{-1}(\mathring{\Gamma}_\lambda), \tag{8.8d}$$

with $\bar{\Phi}^{[2-]\omega} : \mathbb{R} \to \mathbb{R}^{2n+2}$, $h \overset{\mathrm{d}}{\mapsto} (\Phi^{[2]}(\omega, -h), h)$ *and* $U_\omega := \left(\bar{\Phi}^{[2-]\omega}\right)^{-1}(\Omega \times \mathbb{R})$.

Proof. Since the first statement is obvious, we are concerned with the second statement and prove (8.7). This is clear for $i \in \{1, 2, 4\}$ because the conditions that $(\omega, h) \in \Omega \times \mathbb{R}$ and $\Phi^{[i]}(\omega, h) \in \Omega$ are equivalent to the conditions that $\omega \in \Omega$ and $h \in \left(\Phi^{[i]\omega}\right)^{-1}(\Omega)$ (notice that $\Phi^{[i]\omega}$ is defined on whole $\mathbb{R}$ for $i \in \{1, 2, 4\}$). Here, obviously, $\Omega^{[4]\prime}$ itself is $\Omega \times \mathbb{R}$ with $\mathring{I}^{[4]\omega} = \mathbb{R}$ $(\forall \omega \in \Omega)$. For $i = 3$, we see that the subset $\Omega^{[3]\prime}$ with (8.8b) [recall (7.5b)] is equivalent to (8.2b) with replacing "$\geq$" by "$>$". Thus the relation $\Omega^{[3]\prime} = \left(\Phi^{[3]}\right)^{-1}(\Omega)$ is deduced from the following equivalences for $(\omega, h) \in \Omega^{[3]}$:

$$\begin{aligned} & \Phi^{[3]}(\omega, h) \in \Omega \\ \Leftrightarrow\ & \Lambda_h(v) \neq 0 \\ \Leftrightarrow\ & \neg[K(v) < K_0 \text{ and } h/\tau = s_\Lambda(K_0/K(v))] \\ \Leftrightarrow\ & [K(v) < K_0 \Rightarrow h/\tau > s_\Lambda(K_0/K(v))]. \end{aligned}$$

For $i = \tilde{3}$, a discussion similar to $i = 3$ can be used to derive (8.7) with (8.8c) [recall (7.5a)] by observing

$$[(\omega, h) \in \Omega^{[\tilde{3}]} \text{ and } \lambda_h(v) \neq 0] \Leftrightarrow (\omega, h) \in \Omega^{[\tilde{3}]\prime}. \tag{8.9}$$

We also see that $\Omega^{[\tilde{3}]\prime} = H^{-1}(\mathring{\Gamma}_\lambda)$, where $\mathring{\Gamma}_\lambda$ (the interior of Γ_λ) is obtained from (7.3) with removing "$=$" from the both "$\leq$" and "$\geq$". For $i = \check{3}$, we proceed as follows. First we define a subset $A := \left(\bar{\Phi}^{[2-]}\right)^{-1}(\Omega^{[\tilde{3}]\prime})$, then $A = \bigcup_{\omega \in \Omega} \left(\{\omega\} \times \left(\bar{\Phi}^{[2-]\omega}\right)^{-1}(\Omega^{[\tilde{3}]\prime})\right)$. Here, using the relation $\Omega^{[\tilde{3}]\prime} = H^{-1}(\mathring{\Gamma}_\lambda)$ obtained above, we have $\left(\bar{\Phi}^{[2-]\omega}\right)^{-1}(\Omega^{[\tilde{3}]\prime}) = \left(H \circ \left(\bar{\Phi}^{[2-]\omega}|U_\omega\right)\right)^{-1}(\mathring{\Gamma}_\lambda)$. Thus $A = \bigcup_{\omega \in \Omega}\{\omega\} \times \mathring{I}^{[\check{3}]\omega} = \Omega^{[\check{3}]\prime}$. Next we show $A = \left(\Phi^{[\check{3}]}\right)^{-1}(\Omega)$. By the definitions of $\Omega^{[\check{3}]}$ and $\Phi^{[\check{3}]}$ we observe that

$$(\omega, h) \in \left(\Phi^{[\check{3}]}\right)^{-1}(\Omega) \tag{8.10a}$$

$$\Leftrightarrow \left[\begin{array}{l} (\omega, h) \in \Omega \times \mathbb{R},\ \bar{\Phi}^{[2-]}(\omega, h) \in \Omega^{[\tilde{3}]}, \text{ and } \lambda_h(v') \neq 0, \\ \text{where } \bar{\Phi}^{[2-]}(\omega, h) \equiv (\omega', h) \equiv (x,\ v', \mathrm{v}, h) \end{array}\right]. \tag{8.10b}$$

Equation (8.10b) is shown, by using (8.9), to be equivalent to $[(\omega, h) \in \Omega \times \mathbb{R}$ and $(\omega', h) \in \Omega^{[\tilde{3}]\prime}]$, which is also equivalent to $(\omega, h) \in \left(\bar{\Phi}^{[2-]}\right)^{-1}(\Omega^{[\tilde{3}]\prime}) = A$. Thus we have shown $\left(\Phi^{[\check{3}]}\right)^{-1}(\Omega) = A$, which completes the proof. □

Therefore, the range of h in which $\Phi_h^{[i]}(\omega)$ is well defined and takes a value in Ω is given by $\mathring{I}^{[i]\omega}$ for arbitrary $\omega \in \Omega$ and $i \in B$. Specifically, for $i \in \{3, \tilde{3}\}$, the region of h is explicitly given for any $\omega = (x,\ v, \mathrm{v})$ by (8.8b) and (8.8c), which are open intervals including 0 for any $K(v)$. Although explicit expressions seem not clear for the other i, we see that an open interval including 0 is always involved in $\mathring{I}^{[i]\omega}$: $\forall \omega \in \Omega$, $\exists \delta > 0$, $(-\delta, \delta) \subset \mathring{I}^{[i]\omega}$. Regarding $i \in \{1, 2, 4\}$, this holds true, because $\mathring{I}^{[i]\omega}$ becomes an open set due to the fact that $\Phi^{[i]\omega}$ is continuous and Ω is open in $\mathbb{R}^{2n+1}$ and because $0 \in \mathring{I}^{[i]\omega}$ due to the fact that $\Phi^{[i]}(\omega, 0) = \omega$ for all $\omega \in \Omega$. A similar reason is valid for $i = \check{3}$ via (8.8d) [note that U_ω is open and $\bar{\Phi}^{[2-]\omega}(0) = (\omega, 0)$ for any $\omega \in \Omega$]. These results indicate that for any $\omega \in \Omega$ a sufficiently small $|h|$ always applies for $\Phi_h^{[i]}(\omega)$ to be well defined and to take a value in Ω.

Below, we restrict the domain of the definition of $\Phi^{[i]}$ from $\Omega^{[i]}$ into $\Omega^{[i]\prime}$, having the well-defined mapping

$$\Phi^{[i]} : \Omega \times \mathbb{R} \supset \Omega^{[i]\prime} \to \Omega,\ (\omega, h) \mapsto \Phi_h^{[i]}(\omega) \tag{8.11}$$

for all $i \in B$. Next, we consider their composition, in which we have to consider the following three issues. To state the first issue, suppose a two-map composition,

$$\Phi_h(\omega) \equiv (\Phi_h^{[j]} \circ \Phi_h^{[i]})(\omega). \tag{8.12}$$

Even if $\omega' \equiv \Phi_h^{[i]}(\omega) \in \Omega$, equation (8.12) is not necessarily well defined, since $(\omega', h) \in \{\omega'\} \times \mathring{I}^{[j]\omega'}$ may not be ensured. We have to ensure $h \in \mathring{I}^{[j]\omega'}$. However, this cannot be accomplished by simply using $h_{\rm s}$ that is smaller than h such that $h_{\rm s} \in \mathring{I}^{[j]\omega'}$, because ω' should be changed into $\omega'_{\rm s} \equiv \Phi_{h_{\rm s}}^{[i]}(\omega)$ due to this change of the unit timestep, so that $\mathring{I}^{[j]\omega'}$ be changed into $\mathring{I}^{[j]\omega'_{\rm s}}$, which does not ensure $h_{\rm s} \in \mathring{I}^{[j]\omega'_{\rm s}}$. Second, we wish to consider the behavior of $\Phi_h(\omega)$ with varying h (in a continuous manner) in a certain interval J. For example, (4.8)–(4.10) correspond to this kind of issue. Thus we have to ensure the well-definedness of the map such as (8.12), not only for one value h but also for all $h \in J$. Third, we should take into account the composition of any finite number of the maps, generally represented as

$$\Phi_{\mathcal{I}}(\omega, h) \equiv \Phi_{\mathcal{I},h}(\omega) \equiv \left(\Phi_h^{[i_n]} \circ \cdots \circ \Phi_h^{[i_1]}\right)(\omega), \tag{8.13}$$

where $\mathcal{I} \equiv \{i_1, \ldots i_n\} \subset B$, rather than the composition of two maps.

The solution to these issues is demonstrated as follows. The well-definedness of (8.13) can be formulated inductively with respect to n, and it is shown, by induction, to be equivalent to

$$(\omega, h) \in \bigcap_{m=0}^{n-1} \left(\bar{\Phi}^{[i_1]}\right)^{-1} \left(\left(\bar{\Phi}^{[i_2]}\right)^{-1} \left(\cdots \left(\bar{\Phi}^{[i_m]}\right)^{-1} \left(\Omega^{[i_{m+1}]\prime}\right) \cdots\right)\right) =: \Omega'_n, \tag{8.14}$$

where

$$\bar{\Phi}^{[i]} : \Omega^{[i]\prime} \to \Omega \times \mathbb{R},\ (\omega, h) \overset{\rm d}{\mapsto} \left(\Phi^{[i]}(\omega, h),\ h\right) \tag{8.15}$$

for $i \in B$ (note $\Omega'_1 := \Omega^{[i_1]\prime}$). We can then show

$$\forall \omega \in \Omega,\ \exists \delta_{\mathcal{I}} > 0,\ \forall h \in J_{\mathcal{I}} \equiv (-\delta_{\mathcal{I}}, \delta_{\mathcal{I}}),\ (\omega, h) \in \Omega'_n. \tag{8.16}$$

Equation (8.16) can be proved by using the following issues for every $i \in B$: the continuity of $\Phi^{[i]}$, the form of its domain of definition (which is an open set) represented by (8.7), the property of $\mathring{I}^{[i]\omega}$ (i.e., it is an open set including 0), and the relation such that $\Phi^{[i]}(\omega, 0) = \omega$ ($\forall \omega \in \Omega$). Therefore, (8.13) for arbitrary $\omega \in \Omega$ is always well defined for every h in a certain interval $J_{\mathcal{I}}$ around $h = 0$. This is the solution and the basis for our analysis stated below.

8.2. Proof of (4.8)–(4.10) and (4.12). The quantities described in (3.26), (4.4)–(4.6), and (4.11) are now read as maps defined by

$$\Phi : \Omega \times \mathbb{R} \supset \Omega'_{\Phi} \to \Omega,\ (\omega, h) \overset{\mathrm{d}}{\mapsto} \Phi_h(\omega) = \left(\Phi_h^{[4]} \circ \Phi_h^{[3]} \circ \Phi_h^{[2]} \circ \Phi_h^{[1]}\right)(\omega),$$

$$\tilde{\Phi} : \Omega \times \mathbb{R} \supset \Omega'_{\tilde{\Phi}} \to \Omega,\ (\omega, h) \overset{\mathrm{d}}{\mapsto} \tilde{\Phi}_h(\omega) = \left(\Phi_h^{[4]} \circ \tilde{\Phi}_h^{[3]} \circ \Phi_h^{[2]} \circ \Phi_h^{[1]}\right)(\omega),$$

$$\Phi_{\mathrm{M1m}} : \Omega \times \mathbb{R} \supset \Omega'_{\Phi_{\mathrm{M1m}}} \to \Omega,\ (\omega, h) \overset{\mathrm{d}}{\mapsto} \Phi_{\mathrm{M1m},h}(\omega) = \left(\Phi_h^{[4]} \circ \Phi_h^{[1]} \circ \tilde{\Phi}_h^{[3]} \circ \Phi_h^{[2]}\right)(\omega),$$

$$\Phi_{\mathrm{M1}} : \Omega \times \mathbb{R} \supset \Omega'_{\Phi_{\mathrm{M1}}} \to \Omega,\ (\omega, h) \overset{\mathrm{d}}{\mapsto} \Phi_{\mathrm{M1},h}(\omega) = \left(\Phi_h^{[4]} \circ \Phi_h^{[1]} \circ \check{\Phi}_h^{[3]} \circ \Phi_h^{[2]}\right)(\omega),$$

$$\Phi_{\mathrm{M2}} : \Omega \times \mathbb{R} \supset \Omega'_{\Phi_{\mathrm{M2}}} \to \Omega,\ (\omega, h) \overset{\mathrm{d}}{\mapsto} \Phi_{\mathrm{M2},h}(\omega) = \left(\Phi_h^{[4]} \circ \tilde{\Phi}_h^{[3]} \circ \Phi_{h/2}^{[2]} \circ \Phi_h^{[1]} \circ \Phi_{h/2}^{[2]}\right)(\omega),$$

where Ω'_{Φ}, $\Omega'_{\tilde{\Phi}}$, and so on are open sets in $\mathbb{R}^{2n+2}$ defined individually by (8.14); a justification for $\Phi_{\mathrm{M2},h}(\omega)$, which also uses $h/2$, can also be done similarly [e.g., define $\Phi_h^{[2']} := \Phi_{h/2}^{[2]}$, which is $\Phi_h^{[2]}$ using $2\mathbf{M}$ instead of $\mathbf{M}$]. In particular, for any $\omega \in \Omega$, $\exists \delta > 0$, for all $h \in J = (-\delta, \delta)$, the quantities, $\Phi_h(\omega)$, $\tilde{\Phi}_h(\omega)$, and so on, are simultaneously well defined [Take the intersection for the individual maps, $J = \bigcap_{\mathcal{I}} J_{\mathcal{I}}$, in (8.16)]. Now we show that they are all equivalent in the first order. We here define exactly a relation between any two maps $\Phi^{(1)}$ and $\Phi^{(2)}$ in $\mathcal{A} \equiv \{\Phi, \tilde{\Phi}, \Phi_{\mathrm{M1m}}, \Phi_{\mathrm{M1}}, \Phi_{\mathrm{M2}}\}$:

Definition 8.2. *$\Phi^{(1)}$ and $\Phi^{(2)}$ are equivalent in the first order if $\forall \omega \in \Omega$, $\exists \delta > 0$, $\forall h \in (-\delta, \delta)$, $\Phi^{(1)}(\omega, h)$ and $\Phi^{(2)}(\omega, h)$ are well defined and if $\Phi^{(1)}(\omega, h) - \Phi^{(2)}(\omega, h) = \mathcal{O}(h^2)$ $((-\delta, \delta) \ni h \to 0)$ holds. Then we denote $\Phi^{(1)} \sim \Phi^{(2)}$.*

Below we prove the equivalence,

$$\Phi_{\mathrm{M1}} \underset{\mathrm{P8.7}}{\sim} \Phi_{\mathrm{M1m}} \underset{\mathrm{P8.8}}{\sim} \Phi \underset{\mathrm{P8.10}}{\sim} \tilde{\Phi} \underset{\mathrm{P8.11}}{\sim} \Phi_{\mathrm{M2}}, \tag{8.17}$$

where e.g., $\Phi_{\mathrm{M1}} \underset{\mathrm{P8.7}}{\sim} \Phi_{\mathrm{M1m}}$ designates that $\Phi_{\mathrm{M1}} \sim \Phi_{\mathrm{M1m}}$ is shown in Proposition 8.7. Since "$\sim$" becomes an equivalent relation in $\mathcal{A}$, equation (8.17) implies that any two maps in $\mathcal{A}$ are equivalent in the first order, which validates (4.8)–(4.10) and (4.12). In addition, we reconsider (4.1) and (4.2) in Remarks 8.6 and 8.9, respectively. Before proving these issues, we prepare the following lemma:

Lemma 8.3. *Let g_i be a twice-differentiable map ($i = 1, 2$) from $I \subset \mathbb{R}$, which is an open interval including 0, to $\mathbb{R}^n$, satisfying*

$$g_i(h) = \mathcal{O}(h) \quad (I \ni h \to 0). \tag{8.18}$$

Given $v \in \mathbb{R}^n_{\times}$ and put $r_0 \equiv K_0/K(v) \in \mathbb{R}_+$. For $i = 1, 2$, let R_i be a twice-differentiable map from $\Gamma_i \subset \mathbb{R}_+ \times \mathbb{R}$, which is an open set including $(r_0, 0)$, to $\mathbb{R}$, satisfying the following conditions:

$$R_1(r_0, 0) = R_2(r_0, 0), \tag{8.19a}$$

$$D_1 R_1(r_0, 0) = D_1 R_2(r_0, 0) = 0, \tag{8.19b}$$

$$D_2 R_1(r_0, 0) = D_2 R_2(r_0, 0). \tag{8.19c}$$

Then, there exists $\delta > 0$ such that for all $h \in J \equiv (-\delta, \delta)$, $R_1(K_0/K(v + g_1(h)), h/\tau)$ and $R_2(K_0/K(v + g_2(h)), h/\tau)$ are well defined, and

$$R_1\left(\frac{K_0}{K(v + g_1(h))}, \frac{h}{\tau}\right) = R_2\left(\frac{K_0}{K(v + g_2(h))}, \frac{h}{\tau}\right) + \mathcal{O}(h^2) \quad (J \ni h \to 0). \tag{8.20}$$

Proof. Put $f_i^v : I \to \mathbb{R}^n, h \mapsto v + g_i(h)$ for $i = 1, 2$. Then $\varphi_i : I \supset B_i \equiv (f_i^v)^{-1}(\mathbb{R}^n_\times) \to \mathbb{R}^2, h \mapsto (K_0/K(f_i^v(h)), h/\tau)$ is well defined and twice-differentiable. Thus, for all $h \in C := (\varphi_1)^{-1}(\Gamma_1) \cap (\varphi_2)^{-1}(\Gamma_2)$, $(R_i \circ \varphi_i)(h) = R_i(K_0/K(v + g_i(h)), h/\tau)$ is well defined for $i = 1, 2$. Due to the assumptions, C becomes an open set in $\mathbb{R}$. In addition, $C \ni 0$ holds, since the fact that $g_i(0) = \exists \lim_{h\to 0} g_i(h) = 0$, which follows from the continuity of g_i and equation (8.18), leads to $f_i^v(0) = v \in \mathbb{R}^n_\times$, so that $B_i \ni 0$ and $\varphi_i(0) = (K_0/K(f_i^v(0)), 0) = (r_0, 0) \in \Gamma_i$ for both $i = 1$ and 2. Hence, there exists $\delta > 0$ such that $J \equiv (-\delta, \delta) \subset C$, so that for all $h \in J$, $G_i(h) := (R_i \circ \varphi_i)(h)$ is well defined for $i = 1, 2$. Since G_i is twice differentiable, we have $G_i(h) = G_i(0) + DG_i(0)h + \mathcal{O}(h^2)$ $(J \ni h \to 0)$. Thus, if we confirm

$$G_1(0) = G_2(0), \tag{8.21a}$$

$$DG_1(0) = DG_2(0), \tag{8.21b}$$

then we complete the proof. Now, from $G_i(0) = R_i(\varphi_i(0)) = R_i(r_0, 0)$ and from (8.19a), equation (8.21a) is valid. From the relation that $DG_i(0) = D_1R_i(r_0, 0)D\varphi_i^1(0) + D_2R_i(r_0, 0)D\varphi_i^2(0)$, where $\varphi_i \equiv (\varphi_i^1, \varphi_i^2)$, and from (8.19b), we get $DG_i(0) = D_2R_i(r_0, 0)/\tau$ for $i = 1, 2$. Thus (8.21b) follows from (8.19c). □

This Lemma leads to the following two corollaries used in propositions below.

COROLLARY 8.4. *Let $c \in \mathbb{R}^n$ and $v \in \mathbb{R}^n_\times$. Then there exists $\delta > 0$ such that*

$$\lambda_h(v + hc) = \lambda_h(v) + \mathcal{O}(h^2) \quad ((-\delta, \delta) \ni h \to 0). \tag{8.22}$$

Proof. Apply Lemma 8.3 via substituting $g_1 : I \equiv \mathbb{R} \to \mathbb{R}^n, h \overset{\mathrm{d}}{\mapsto} hc$, $g_2 : \mathbb{R} \to \mathbb{R}^n, h \overset{\mathrm{d}}{\mapsto} 0$, and $R_1 \equiv R_2 \equiv \lambda|\mathring{\Gamma}_\lambda : \Gamma_1 \equiv \Gamma_2 \equiv \mathring{\Gamma}_\lambda \to \mathbb{R}$, which is defined in (7.1). Then $(r_0, 0) \in \mathring{\Gamma}_\lambda$, and the required conditions, including (8.18) and (8.19), are easily verified to be met. Thus $R_1(K_0/K(v + g_1(h)), h/\tau) = \lambda_h(v + hc)$ and $R_2(K_0/K(v + g_2(h)), h/\tau) = \lambda_h(v)$ for $h \in J \equiv (-\delta, \delta)$ follow (8.20) to indicate (8.22). □

COROLLARY 8.5. *Let g be a twice-differentiable map from $I \subset \mathbb{R}$, which is an open interval including 0, to $\mathbb{R}^n$, satisfying*

$$g(h) = \mathcal{O}(h^2) \quad (I \ni h \to 0).$$

Let $b \in \mathbb{R}^n$ and $v \in \mathbb{R}^n_\times$. Then there exists $\delta > 0$ such that

$$\Lambda_h(v + hb + g(h)) = \lambda_h(v + hb + g(h)) + \mathcal{O}(h^2) \quad ((-\delta, \delta) \ni h \to 0). \tag{8.23}$$

Proof. Apply Lemma 8.3 via substituting $g_1 \equiv g_2 : I \to \mathbb{R}^n, h \overset{\mathrm{d}}{\mapsto} g(h) + hb$, $R_1 \equiv \Lambda|\mathring{\Gamma}_\Lambda : \Gamma_1 \equiv \mathring{\Gamma}_\Lambda \to \mathbb{R}$ defined in (7.2), and $R_2 \equiv \lambda|\mathring{\Gamma}_\lambda : \Gamma_2 \equiv \mathring{\Gamma}_\lambda \to \mathbb{R}$ defined in (7.1). Then $(r_0, 0) \in \mathring{\Gamma}_\Lambda, \mathring{\Gamma}_\lambda$, and the required conditions, including (8.18) and (8.19), are met. Thus $R_1(K_0/K(v + g_1(h)), h/\tau) = \Lambda_h(v + hb + g(h))$ and $R_2(K_0/K(v + g_2(h)), h/\tau) = \lambda_h(v + hb + g(h))$ for $h \in J \equiv (-\delta, \delta)$ follow (8.20). □

REMARK 8.6. *For any $v \in \mathbb{R}^n_\times$, as obtained from Corollary 8.5 with $b \equiv 0$ and $g \equiv 0$, there exists $\delta > 0$ such that*

$$\Lambda_h(v) = \lambda_h(v) + \mathcal{O}(h^2) \quad ((-\delta, \delta) \ni h \to 0), \tag{8.24}$$

and so

$$\Lambda_{\tau s}(v) = \lambda_{\tau s}(v) + \mathcal{O}(s^2) \quad ((-\delta/\tau, \delta/\tau) \ni s \to 0). \tag{8.25}$$

Equations (8.24) and (8.25) correspond to the accurate expressions of (4.1a) and (4.1b), respectively.

Now, we prove (8.17) via the following four propositions.

PROPOSITION 8.7. *$\Phi_{M1} \sim \Phi_{M1m}$ holds true.*

Proof. For any $\omega = (x, v, \mathrm{v}) \in \Omega$, we know $\Phi_{\mathrm{M1m},h}(\omega)$ and $\Phi_{\mathrm{M1},h}(\omega)$ are well defined for all h in a certain interval $J' \equiv (-\delta', \delta')$ and obtain

$$\left(\tilde{\Phi}_h^{[3]} \circ \Phi_h^{[2]}\right)(\omega) - \left(\check{\Phi}_h^{[3]} \circ \Phi_h^{[2]}\right)(\omega) \tag{8.26a}$$

$$= (0, [\lambda_h(v + hc_x) - \lambda_h(v)](v + hc_x), 0) \in \mathbb{R}^{2n+1} \tag{8.26b}$$

for all $h \in J'$, where $c_x \equiv F(x)\mathbf{M}^{-1} \in \mathbb{R}^n$. In (8.26b), applying Corollary 8.4, we have $\lambda_h(v + hc_x) - \lambda_h(v) = \mathcal{O}(h^2)$ $((-\delta'', \delta'') \ni h \to 0)$. Thus,

$$\begin{aligned}
&\left(\tilde{\Phi}_h^{[3]} \circ \Phi_h^{[2]}\right)(\omega) - \left(\check{\Phi}_h^{[3]} \circ \Phi_h^{[2]}\right)(\omega) \\
&= \big(0, \mathcal{O}(h^2)(v + hc_x), 0\big) \\
&= \mathcal{O}(h^2) \quad (I \ni h \to 0),
\end{aligned}$$

where $I \equiv (-\delta, \delta)$ with $\delta \equiv \min\{\delta', \delta''\} > 0$. Noting that $\Phi_{\mathrm{M1m},h}(\omega) = \Psi(\varpi(h) + \varphi(h), h)$ and $\Phi_{\mathrm{M1},h}(\omega) = \Psi(\varpi(h), h)$ for $h \in I$, where maps $\varpi : I \to \Omega, h \overset{\mathrm{d}}{\mapsto} \left(\check{\Phi}_h^{[3]} \circ \Phi_h^{[2]}\right)(\omega)$, $\varphi : I \to \mathbb{R}^{2n+1}, h \overset{\mathrm{d}}{\mapsto} \left(\tilde{\Phi}_h^{[3]} \circ \Phi_h^{[2]}\right)(\omega) - \left(\check{\Phi}_h^{[3]} \circ \Phi_h^{[2]}\right)(\omega)$, and $\Psi : \Omega_2' \to \Omega, (\omega, h) \overset{\mathrm{d}}{\mapsto} \left(\Phi_h^{[4]} \circ \Phi_h^{[1]}\right)(\omega)$ [see (8.14)], are twice-differentiable, we have $\Phi_{\mathrm{M1m},h}(\omega) - \Phi_{\mathrm{M1},h}(\omega) = \Psi(\varpi(h) + \mathcal{O}(h^2), h) - \Psi(\varpi(h), h) = \mathcal{O}(h^2)$ $(I \ni h \to 0)$. □

PROPOSITION 8.8. *$\Phi_{M1m} \sim \Phi$ holds true.*

Proof. For any $\omega = (x, v, \mathrm{v}) \in \Omega$, it is shown that $\Phi_{\mathrm{M1m},h}(\omega)$, $\Phi_h(\omega)$, and

$$\hat{\Phi}_h(\omega) \equiv \left(\Phi_h^{[4]} \circ \Phi_h^{[1]} \circ \Phi_h^{[3]} \circ \Phi_h^{[2]}\right)(\omega) \tag{8.27}$$

are well defined for all h in a certain $J' \equiv (-\delta', \delta')$ and

$$\left(\tilde{\Phi}_h^{[3]} \circ \Phi_h^{[2]}\right)(\omega) - \left(\Phi_h^{[3]} \circ \Phi_h^{[2]}\right)(\omega) \tag{8.28a}$$

$$= (0, [\lambda_h(v + hc_x) - \Lambda_h(v + hc_x)](v + hc_x), 0) \in \mathbb{R}^{2n+1} \tag{8.28b}$$

holds for $\forall h \in J'$, where $c_x \equiv F(x)\mathbf{M}^{-1} \in \mathbb{R}^n$. Applying Corollary 8.5 with $g \equiv 0$ to (8.28b), we have $\delta'' \in (0, \delta']$ such that

$$\left(\tilde{\Phi}_h^{[3]} \circ \Phi_h^{[2]}\right)(\omega) - \left(\Phi_h^{[3]} \circ \Phi_h^{[2]}\right)(\omega) \tag{8.29a}$$

$$= \mathcal{O}(h^2) \quad (J \equiv (-\delta'', \delta'') \ni h \to 0). \tag{8.29b}$$

Thus, using a similar manner (replacing $\check{\Phi}^{[3]}$ with $\Phi^{[3]}$) in the proof of Proposition 8.7, on the basis of the smoothness of the maps, we get

$$\Phi_{\mathrm{M1m},h}(\omega) - \hat{\Phi}_h(\omega) = \mathcal{O}(h^2) \ (J \ni h \to 0). \tag{8.30}$$

Since both $\hat{\Phi}_h$ and Φ_h are first-order integrators, there exits $\delta \in (0, \delta'']$ such that for $I \equiv (-\delta, \delta)$,

$$\hat{\Phi}_h(\omega) - \Phi_h(\omega) = \mathcal{O}(h^2) \quad (I \ni h \to 0). \tag{8.31}$$

Equations (8.30) and (8.31) imply $\Phi_{\mathrm{M1m},h}(\omega) - \Phi_h(\omega) = \mathcal{O}(h^2)$ $(I \ni h \to 0)$. □

REMARK 8.9. *We can apply the identically zero force, $F \equiv 0$, then $\Phi_h^{[2]}$ becomes an identity map on Ω, so that (8.29) indicates (4.2).*

PROPOSITION 8.10. *$\Phi \sim \tilde{\Phi}$ holds true.*

Proof. For any $\omega = (x, v, \mathrm{v}) \in \Omega$ and for all h in a certain $J \equiv (-\delta', \delta')$, $\tilde{\Phi}_h(\omega)$ and $\Phi_h(\omega)$ are well defined, and

$$\left(\Phi_h^{[2]} \circ \Phi_h^{[1]}\right)(\omega) \tag{8.32a}$$

$$= \left(x + hv,\, hF(x + hv)\mathbf{M}^{-1} + v,\, \mathrm{v}\right) \tag{8.32b}$$

$$= \left(x + hv,\, hF(x)\mathbf{M}^{-1} + g(h) + v,\, \mathrm{v}\right), \tag{8.32c}$$

with $g : J \to \mathbb{R}$, $h \overset{\mathrm{d}}{\mapsto} h(F(x + hv) - F(x))\mathbf{M}^{-1}$. Since g is twice differentiable and $g(h) = h\,\mathcal{O}(h) = \mathcal{O}(h^2)$ $(J \ni h \to 0)$, by applying Corollary 8.5 to (8.32c), we have $\delta \in (0, \delta']$ such that for $h \in I \equiv (-\delta, \delta)$,

$$\begin{aligned}
&\left(\Phi_h^{[3]} \circ \Phi_h^{[2]} \circ \Phi_h^{[1]}\right)(\omega) \\
&= \left(x + hv,\, \Lambda_h(v + hF(x)\mathbf{M}^{-1} + g(h))(v + hF(x)\mathbf{M}^{-1} + g(h)),\, \mathrm{v}\right) \\
&= \left(x + hv,\, (\lambda_h(v + hF(x)\mathbf{M}^{-1} + g(h)) + \mathcal{O}(h^2)))(v + hF(x)\mathbf{M}^{-1} + g(h)),\, \mathrm{v}\right) \quad (I \ni h \to 0) \\
&= \left(x + hv,\, (\lambda_h(v + hF(x)\mathbf{M}^{-1} + g(h)))(v + hF(x)\mathbf{M}^{-1} + g(h)),\, \mathrm{v}\right) + \mathcal{O}(h^2) \\
&= \left(\tilde{\Phi}_h^{[3]} \circ \Phi_h^{[2]} \circ \Phi_h^{[1]}\right)(\omega) + \mathcal{O}(h^2).
\end{aligned}$$

Thus, from the smoothness of the maps, we have $\Phi_h^{[4]}\left(\left(\Phi_h^{[3]} \circ \Phi_h^{[2]} \circ \Phi_h^{[1]}\right)(\omega)\right) = \Phi_h^{[4]}\left(\left(\tilde{\Phi}_h^{[3]} \circ \Phi_h^{[2]} \circ \Phi_h^{[1]}\right)(\omega)\right) + \mathcal{O}(h^2)$ $(I \ni h \to 0)$, indicating

$$\tilde{\Phi}_h(\omega) = \Phi_h(\omega) + \mathcal{O}(h^2) \quad (I \ni h \to 0). \tag{8.33}$$

□

PROPOSITION 8.11. *$\tilde{\Phi} \sim \Phi_{M2}$ holds true.*

Proof. For any $\omega = (x, v, \mathrm{v}) \in \Omega$ and for all h in a certain $I \equiv (-\delta, \delta)$, $\tilde{\Phi}_h(\omega)$ and $\Phi_{\mathrm{M2},h}(\omega)$ are well defined, and

$$\begin{aligned}
&\left(\Phi_h^{[2]} \circ \Phi_h^{[1]}\right)(\omega) - \left(\Phi_{h/2}^{[2]} \circ \Phi_h^{[1]} \circ \Phi_{h/2}^{[2]}\right)(\omega) \\
&= \left(-\tfrac{h^2}{2}F(x)\mathbf{M}^{-1},\, hF(x + hv)\mathbf{M}^{-1} - \tfrac{h}{2}F(x + hv + \tfrac{h^2}{2}F(x)\mathbf{M}^{-1})\mathbf{M}^{-1} - \tfrac{h}{2}F(x)\mathbf{M}^{-1},\, 0\right) \\
&= \left(\mathcal{O}(h^2),\, hF(x)\mathbf{M}^{-1} + \mathcal{O}(h^2) - \tfrac{h}{2}(F(x) + \mathcal{O}(h))\mathbf{M}^{-1} - \tfrac{h}{2}F(x)\mathbf{M}^{-1},\, 0\right) \quad (I \ni h \to 0) \\
&= \mathcal{O}(h^2).
\end{aligned}$$

Thus, from the smoothness of the maps, we get $\left(\Phi_h^{[4]} \circ \tilde{\Phi}_h^{[3]}\right)\left(\left(\Phi_h^{[2]} \circ \Phi_h^{[1]}\right)(\omega)\right) = \left(\Phi_h^{[4]} \circ \tilde{\Phi}_h^{[3]}\right)\left(\left(\Phi_{h/2}^{[2]} \circ \Phi_h^{[1]} \circ \Phi_{h/2}^{[2]}\right)(\omega)\right) + \mathcal{O}(h^2)$ $(I \ni h \to 0)$, indicating

$$\tilde{\Phi}_h(\omega) = \Phi_{\mathrm{M2},h}(\omega) + \mathcal{O}(h^2) \quad (I \ni h \to 0). \tag{8.34}$$

□

ACKNOWLEDGMENTS. This work was supported by a Grant-in-Aid for Scientific Research (C) (25390156) from JSPS and the "Development of core technologies for innovative drug development based upon IT" from Japan Agency for Medical Research and development, AMED.

REFERENCES

[1] W. G. Hoover, *Computational Statistical Mechanics*, Elsevier, Amsterdam, 1991.
[2] R. Skeel, *What makes molecular dynamics work?*, SIAM J. Sci. Comput., 31 (2009), pp. 1363-1378.
[3] M. Allen and D. Tildesley, *Computer simulation of liquids*, Oxford, New York, 2002.
[4] T. Schlick, *Molecular modeling and simulation: an interdisciplinary guide*, Springer Science & Business Media, New York, 2010.
[5] S. Nosé, *Constant temperature molecular-dynamics methods*, Prog. Theor. Phys. Suppl., 103 (1991), pp. 1-46.
[6] P. H. Hünenberger, *Thermostat algorithms for molecular dynamics simulations*, in Advanced Computer Simulation: Approaches for Soft Matter Sciences I., C. Holm and K. Kremer, eds., Springer, Berlin, 2005, pp. 105-149.
[7] O. G. Jepps and L. Rondoni, *Deterministic thermostats, theories of nonequilibrium systems and parallels with the ergodic condition*, J. Phys. A, 43 (2010), pp. 133001.
[8] S. Nosé, *A unified formulation of the constant temperature molecular dynamics methods*, J. Chem. Phys., 81 (1984), pp. 511.
[9] W. Hoover, *Canonical dynamics: Equilibrium phase-space distributions*, Phys. Rev. A, 31 (1985), pp. 1695-1697.
[10] S. Pieprzyk, D. M. Heyes, S. Maćkowiak and A. C. Brańka, *Galilean-invariant Nosé-Hoover-type thermostats*, Phys. Rev. E, 91 (2015), pp. 03331.
[11] I. Fukuda and K. Moritsugu, *Coupled Nosé-Hoover equations of motion to implement a fluctuating heat-bath temperature*, Phys. Rev. E, 93 (2016), pp. 033306.
[12] B. Leimkuhler and X. Shang, *Adaptive thermostats for noisy gradient systems*, SIAM J. Sci. Comput., 38 (2016), pp. A712-A736.
[13] I. Fukuda, *Coupled Nosé-Hoover lattice: A set of the Nosé-Hoover equations with different temperatures*, Phys. Lett. A, 380 (2016), pp. 2465-2474.
[14] W. G. Hoover, J. C. Sprott and P. K. Patra, *Ergodic time-reversible chaos for Gibbs' canonical oscillator*, Phys. Lett. A, 379 (2015), pp. 2935-2940.
[15] W. G. Hoover, *Molecular dynamics*, Springer-Verlag, Berlin, 1986.
[16] W. G. Hoover, A. J. C. Ladd and B. Moran, *High-strain-rate plastic flow studied via nonequilibrium molecular dynamics*, Phys. Rev. Lett., 48 (1982), pp. 1818-1820.
[17] D. J. Evans, *Computer "experiment" for nonlinear thermodynamics of Couette flow*, J. Chem. Phys., 78 (1983), pp. 3297-3302.
[18] D. J. Evans, W. G. Hoover, B. H. Failor, B. Moran and A. J. C. Ladd, *Nonequilibrium molecular dynamics via Gauss's principle of least constraint*, Phys. Rev. A, 28 (1983), pp. 1016-1021.
[19] D. J. Evans and G. P. Morriss, *The isothermal/isobaric molecular dynamics ensemble*, Phys. Lett. A, 98 (1983), pp. 433-436.
[20] H. J. C. Berendsen, J. P. M. Postma, W. F. Van Gunsteren, A. Dinola and J. R. Haak, *Molecular dynamics with coupling to an external bath*, J. Chem. Phys., 81 (1984), pp. 3684-3690.
[21] T. Morishita, *Fluctuation formulas in molecular-dynamics simulations with the weak coupling heat bath*, J. Chem. Phys., 113 (2000), pp. 2976-2982.
[22] H. J. C. Berendsen, D. Van Der Spoel and R. Van Drunen, *GROMACS: A message-passing parallel molecular dynamics implementation*, Comput. Phys. Commun., 91 (1995), pp. 43-56.
[23] H. Eslami, F. Mojahedi and J. Moghadasi, *Molecular dynamics simulation with weak coupling to heat and material baths*, J. Chem. Phys., 133 (2010), pp. 084105.
[24] S. A. Moga, N. Goga and A. Hadar, *Combining Berendsen thermostat with dissipative particle dynamics (DPD) for polymer simulation*, Materiale Plastice, 50 (2013), pp. 196-200.
[25] G. Bussi, D. Donadio and M. Parrinello, *Canonical sampling through velocity rescaling*, J. Chem. Phys., 126 (2007), pp. 014101.
[26] J. E. Basconi and M. R. Shirts, *Effects of temperature control algorithms on transport proper-*

ties and kinetics in molecular dynamics simulations, J. Chem. Theory Comput., 9 (2013), pp. 2887-2899.

[27] D. Okunbor and R. D. Skeel, *Explicit canonical methods for Hamiltonian-systems*, Math. Comp., 59 (1992), pp. 439-455.

[28] J.-M. Sanz-Serna and M.-P. Calvo, *Numerical Hamiltonian problems,* Chapman & Hall, London, 1994.

[29] R. D. Ruth, *A canonical integration technique*, IEEE Trans. Nucl. Sci., 30 (1983), pp. 2669-2671.

[30] H. Yoshida, *Construction of higher order symplectic integrators*, Phys. Lett. A, 150 (1990), pp. 262-268.

[31] R. I. Mclachlan and P. Atela, *The accuracy of symplectic integrators*, Nonlinearity, 5 (1992), pp. 541-562.

[32] J. M. Sanz-Serna, *Symplectic integrators for Hamiltonian problems: an overview*, Acta Numer., 1 (1992), pp. 243-286.

[33] R. Skeel, G. Zhang and T. Schlick, *A Family of Symplectic Integrators: Stability, Accuracy, and Molecular Dynamics Applications*, SIAM J. Sci. Comput., 18 (1997), pp. 203-222.

[34] M. Tuckerman, B. J. Berne and G. J. Martyna, *Reversible multiple time scale molecular dynamics*, J. Chem. Phys., 97 (1992), pp. 1990-2001.

[35] A. Dullweber, B. Leimkuhler and R. Mclachlan, *Symplectic splitting methods for rigid body molecular dynamics*, J. Chem. Phys., 107 (1997), pp. 5840-5851.

[36] I. P. Omelyan, I. M. Mryglod and R. Folk, *Algorithm for molecular dynamics simulations of spin liquids*, Phys. Rev. Lett., 86 (2001), pp. 898-901.

[37] I. Fukuda and H. Nakamura, *Construction of an extended invariant for an arbitrary ordinary differential equation with its development in a numerical integration algorithm*, Phys. Rev. E, 73 (2006), pp. 026703.

[38] R. I. McLachlan and G. R. W. Quispel, *Geometric integrators for ODEs*, J. Phys. A, 39 (2006), pp. 5251-5285.

[39] R. I. Mclachlan and G. R. W. Quispel, *Splitting methods*, Acta Numer., 11 (2002), pp. 341–434.

[40] V. L. Golo and K. V. Shaitan, *Dynamic attractor associated with the Berendsen thermostat and slow dynamics of biological macromolecules*, Biophysics, 47 (2002), pp. 567-573.

[41] M. Khalili, A. Liwo, A. Jagielska and H. A. Scheraga, *Molecular dynamics with the united-residue model of polypeptide chains. II. Langevin and Berendsen-Bath dynamics and tests on model α-helical systems*, J. Phys. Chem. B, 109 (2005), pp. 13798-13810.

[42] S. Queyroy, H. Nakamura and I. Fukuda, *Numerical examination of the extended phase-space volume-preserving integrator by the Nosé-Hoover molecular dynamics equations*, J. Comput. Chem., 30 (2009), pp. 1799-815.

[43] E. Hairer, C. Lubich and G. Wanner, *Geometric numerical integration: structure-preserving algorithms for ordinary differential equations*, Springer-Verlag, Berlin, 2002.

[44] R. I. Mclachlan, *On the numerical-integration of ordinary differential-equations by symmetrical composition methods*, SIAM J. Sci. Comput., 16 (1995), pp. 151-168.

[45] S. Blanes and P. C. Moan, *Practical symplectic partitioned Runge-Kutta and Runge-Kutta-Nystrom methods*, J. Comput. Appl. Math., 142 (2002), pp. 313-330.

[46] S. C. Harvey, R. K. Z. Tan and T. E. Cheatham, *The flying ice cube: velocity rescaling in molecular dynamics leads to violation of energy equipartition*, J. Comput. Chem., 19 (1998), pp. 726-740.

[47] M. G. Martin and J. I. Siepmann, *Transferable potentials for phase equilibria. 1. united-atom description of n-alkanes*, J. Phys. Chem. B, 102 (1998), pp. 2569-2577.

[48] S. Blanes, F. Casas and A. Murua, *On the numerical integration of ordinary differential equations by processed methods*, SIAM J. Numer. Anal., 42 (2004), pp. 531-552.

[49] M. Suzuki, *Hybrid exponential product formulas for unbounded operators with possible applications to Monte Carlo simulations*, Phys. Lett. A, 201 (1995), pp. 425-428.

[50] S. A. Chin, *Symplectic integrators from composite operator factorizations*, Phys. Lett. A, 226 (1997), pp. 344-348.

[51] J. Auer, E. Krotscheck and S. A. Chin, *A fourth-order real-space algorithm for solving local Schrödinger equations*, J. Chem. Phys., 115 (2001), pp. 6841-6846.